

Comenius University  
Faculty of Mathematics, Physics and Informatics  
Department of Applied Informatics



# **Complex Networks: dynamics and applications**

by

**Peter Náther**

Supervisor: doc. RNDr. Mária Markošová PhD.

Bratislava, 2010

# Abstract

Many complex networks have similar features which can be described by suitable models. Some of these features are developed during network time evolution. Here I study models which evolve by preferential attachment leading to the scale-free and after certain modifications also to the hierarchical network structure. Methods of complex networks analysis have been applied to the functional brain networks. I have studied these ad-hoc networks to discover differences in the structure of brain networks under different conditions.

# Abstrakt

(in Slovak language)

Mnohé komplexné siete majú podobné vlastnosti. Tieto siete môžeme opísať vhodnými modelmi. Niektoré z vlastností týchto sietí sa menia počas vývoja siete v čase. V tejto práci skúmam modely, ktoré rozvíjajú siete pomocou preferenčného pripájania a vedú tak k sieťam s bezškálovou štruktúrou. Modifikáciou týchto modelov, vieme vytvoriť modely generujúce siete s hierarchickou štruktúrou. Metódy analýzy komplexných sietí som aplikoval pri skúmaní funkčných sietí mozgu. Jedná sa o ad-hoc siete a v mojej práci som sa pokúšal nájsť rozdiely v štruktúre funkčných sietí mozgu vytvorených za rôznych podmienok.

**Kľúčové slová:** funkčné siete mozgu, komplexné siete, modely dynamických systémov

*I would like to thank my supervisor Mária Markošová for her advice and extensive support. My thesis would not have been possible without her and without the encouragement and guidance she has given to me.*

*I would like to express my thanks to my colleagues Boris Rudolf and Ľubica Benušková for their help, advice and great ideas about research and academic life. Thanks to Ľubica Benušková I have spent a great time on the Department of Computer Science at the University of Otago, where part of my research on functional brain networks was done.*

*Finally, I thank my family, my parents, my brother and sister, my friends and colleagues for their support, patience and listening to my endless ridiculous talks about some strange graphs and networks.*

---

# Predhovor

---

Modely komplexných sietí sa úspešne používajú na modelovanie mnohých systémov ako napríklad www, Internet, Facebook či infraštruktúra elektrických rozvodných sietí. Prvé pokusy modelovať takéto systémy spravili matematici Paul Erdős a Alfréd Rényi, ktorí sú autormi klasickej teórie grafov [26]. Ukázalo sa však, že topológia a vývin takýchto systémov sa riadi danými princípmi a štruktúra vzniknutých sietí je odlišná od náhodných grafov. Siete malého sveta (small world), spopularizované experimentom psychológa Stanleyho Milgrama, ktorý tvrdil, že ľubovoľný dvaja ľudia sa navzájom poznajú cez najviac 6 svojich známych a bezškálové siete opísané Barabásim a Albertovou [9] sa stali veľmi populárnymi. Tieto siete sú charakterizované nízkou seperáciou vrcholov, sebedpodobnosťou či odolnosťou voči náhodným útokom. Problémom je, že reálne systémy sú obrovské, rádovo stotisíccky uzlov a milióny hrán, čo mimoriadne sťažuje štúdium týchto sietí. Na zisťovanie vlastností takýchto systémov preto používame modely, ktoré nám pomáhajú predikovať a analyzovať budúci stav a parametre sietí.

V mojej práci sa venujem štúdiu modelov komplexných sietí a možností aplikácii jednotlivých modelov a metód. Zamerám sa na modely inšpirované mechanizmami odpozorovanými na reálnych systémoch. Takéto modely nám pomáhajú lepšie rozumieť procesom vzniku vývoja komplexných. Vďaka nim môžeme taktiež generovať budúcnosť systémov na základne aktuálne nameraných parametrov.

V teoretickej časti mojej práci som spolu s mojimi spolupracovníkmi modifikoval súčasný model navrhnutý Dorogovtsevom a Mendésom [20], generujúci bezškálové siete s dvoma škálovacími režimami. Navrhnutou modifikáciou sme dosiahli možnosť manipulovať škálovacím exponentom vygenerovanej siete, pomocou vstupných parametrov modelu. V reálnych systémoch sa často krát stretávame s hierarchickou štruktúrou sietí [52, 51]. Existujú aj modely sietí generujúce hierarchické siete [51], ale tieto sú založené na inkrementálnom pridávaní deterministického vzoru a tak obmedzujú stochastickosť vygenerovanej siete. Preto sme

vyvinuli stochastický model generujúci generujúci hierarchickú sieť, ktorý nie je ohraničený uvedenými obmedzeniami. Ako vhodný mechanizmus sa opäť ukázalo preferenčné pripájanie, za ktorého základ zoberieme klasterizačný koeficient.

Teória komplexných sietí a metódy ich skúmania sa ukázali byť v mnohých prípadoch vhodným mechanizmom pri riešení reálnych problémov. Aplikovanie na reálne problémy nám navyše častokrát prinesie nový uhol pohľadu a pomáha zlepšiť teoretické modely či algoritmy. V mojej práci som metódy skúmania komplexných sietí aplikoval na výskum v pomerne novej oblasti a tou sú funkčné siete v mozgu založené na meraniach funkčnej magnetickej rezonancie [16]. Uzlami v týchto sieťach sú voxely, malé oblasti mozgu ktoré sú merané počas funkčnej magnetickej rezonancie. Hrana medzi dvoma voxelmi vzniká ak zmena jedného voxelu v čase je v korelácii so zmenou intenzity iného voxelu. V mojej práci analyzujem štruktúru funkčných sietí mozgu z pohľadu sietí malého sveta, bezškálových a hierarchických sietí. Zameral som sa na rozdiely medzi funkčnými sieťami rôznych osôb počas vykonávania jednoduchých kognitívnych úloh. Študoval som taktiež funkčné siete ľudí s anatomickými zmenami mozgovej štruktúry, ktoré vyvoláva demencia. Časť môjho výskumu som realizoval na Department of Computer Science, Univerzity of Otago, Dunedin, New Zealand, vďaka doc. RNDr. Ľubicy Beňuškovéj, PhD. a Dr. Liz Franz, PhD.

---

# Contents

---

<b>Contents</b>	<b>i</b>
<b>1 Introduction</b>	<b>1</b>
1.1 Motivation . . . . .	2
<b>2 Overview</b>	<b>4</b>
2.1 Basics of the graph theory . . . . .	4
2.2 Statistical properties of complex networks . . . . .	5
2.3 Network models . . . . .	8
2.3.1 Random network . . . . .	8
2.3.2 Small world - Watts-Strogatz model . . . . .	9
2.3.3 Preferential attachment - Barabási-Albert model . . . . .	10
2.3.4 Accelerated growth - Dorogovtsev-Mendés model . . . . .	13
2.3.5 Exponential tail . . . . .	14
2.3.6 Hierarchical network model . . . . .	15
2.3.7 Random walk model . . . . .	18
<b>3 Positional word web</b>	<b>21</b>
3.1 Introduction . . . . .	21
3.2 Word web . . . . .	21
3.3 Word web model . . . . .	23
3.4 Numerical studies of the word web . . . . .	25
3.5 Conclusions . . . . .	26
<b>4 Clustering driven model</b>	<b>31</b>
4.1 Introduction . . . . .	31
4.2 The model . . . . .	32
4.3 Results . . . . .	33
4.4 Conclusions . . . . .	38
<b>5 Functional brain networks</b>	<b>43</b>

5.1	Introduction . . . . .	43
5.2	Network construction and analysis . . . . .	44
5.3	Active and resting functional brain networks . . . . .	48
5.3.1	Material and methods . . . . .	49
5.3.2	Results . . . . .	49
5.4	Functional brain networks and dementia . . . . .	53
5.4.1	Material and methods . . . . .	53
5.4.2	Results . . . . .	54
5.5	Conclusions . . . . .	54
<b>6</b>	<b>Conclusions and discussion</b>	<b>58</b>
	<b>Bibliography</b>	<b>62</b>
<b>A</b>	<b>Appendix A</b>	<b>68</b>
<b>B</b>	<b>Appendix B</b>	<b>72</b>

## Chapter 1

---

# Introduction

---

A lot of systems, such as www, the Internet, Facebook, social interactions, chemical reactions, protein interactions or power grid infrastructure are successfully modelled by network models. First attempts to model some of these systems have been done by Hungarian mathematicians Paul Erdős, Alfréd Rényi and Béla Bollobás. In their times random graphs were studied extensively and thus naturally, random graph models were used to describe such systems. Erdős and Rényi are authors of classical random graph theory [26]. However it was soon recognized, that the topology and evolution of these systems are governed by some organizing principles resulting in a structure different from the structure of random graphs. Small-worlds popularized by the "six degree separation" experiment by the psychologist Stanley Milgram (1967), stating that there was a path of acquaintances with typical length about six between most pairs of people in the United States [37] and scale-free networks described by Barabási and Albert [9] becomes very popular. These networks are characterized by a short node separation, self-similarity or robustness to random attacks and failures [5]. However we struggle with the fact that these systems are extremely large with hundreds of thousands of nodes and millions of edges. To study such networks, uncover their behavior and properties is not always feasible. If possible, network models are created and used to predict and analyze future structure and parameters of real networks. Good models with a help of statistical properties of smaller networks allow us to predict the topology and behavior of large networks and simulate algorithms.

## 1.1 Motivation

My interest in studying complex networks is to understand how their structure is influenced by the dynamical processes. The aim is to find models that evolve to the networks with specific statistical properties discovered in real systems. These properties are good to know if we, for example want to build a network with a good communication capability that is resistant to the damage. Here I study models inspired by the mechanism observed in real systems. Such models help us to understand process of network evolution and predict future of the networks based on characteristics for present and past states. Knowledge of these processes, structures and statistical properties can be used to design algorithms that can take advantage of using such information. From the point of view of informatics, a real networks have a lot of good properties. Together with a high resistance for random attacks which is important for communication and computer networks, information about the structure can be effectively used to improve navigation and search algorithms [68, 36]. For example ability to transfer a signal is influenced by the network structure [54] and also by the cooperation of transmitters and receivers [28]. Small world model was used also for improvement of the performance of a peer-to-peer network [67]. Here I put several examples of networks which I have studied in this thesis.

**Positional word web:** Cancho and Solé [15] have studied the positional word web [42]. They have shown that the positional word web has small world and scale-free properties. A generative model for this network was developed by Dorogovtsev and Mendes [20]. However there is some discrepancy between the measured properties and values predicted by models. In Chapter 3 I introduce the model combining the preferential attachment with a node rewiring for better fit of the experimental data. To check the relevance of the model and explain its limits, I have studied numerically positional word web based on the Bible [38].

**Clustering driven model:** Networks with a certain hierarchy among nodes are quite common in real world [52, 51]. However proposed models describing hierarchy creation are not complex enough to capture the process [51]. In chapter 4 I will introduce a random model evolving to the hierarchical network. This model is as a combination of clustering driven preferential attachment and a local rule of adding edges to the neighbourhood [48].

**Functional brain networks:** Analyzing large real networks can answer many questions regarding their structure and evolution. Properties of small world networks are responsible for searchability and navigability of networks [59, 68], scale-free properties points to the self similarity and robustness to the random attacks or failures. Hierarchicity reveals the high level of organization. In chapter 5 I

show an application of network theory. I have studied functional brain networks based on the fMRI data. In my study I analyze small world structure of functional brain networks. I have focused on the differences among the functional brain networks of individual people while performing a different tasks or having some structural anatomical changes of the underlying anatomical structure as it is known by people with dementia.

## Chapter 2

---

# Overview

---

Chapter 2 is devoted to the introduction of necessary terminology and essential well known network models. In the next part I introduce some basic graph theory concepts [18]. Section 2.2 describes most important statistical properties used in studying complex networks. Section 2.3 is left to the models of complex networks [9, 24, 52, 62, 26].

### 2.1 Basics of the graph theory

A network is represented by a graph. Basically, we can say that a graph is a set of nodes connected by a set of edges. However, more formal definition will be useful [18]:

**Definition 1.** *A graph is a pair  $G = (V, E)$  of sets, satisfying  $E \subseteq [V]^2$ ; thus the elements of  $E$  are 2-element subsets of  $V$ . The elements of  $V$  are the vertices or nodes of the graph  $G$  and the elements of  $E$  are its edges.  $N$  denotes the number of nodes,  $N = |V|$  and  $M$  denotes the number of edges  $M = |E|$ , where  $||$  means the cardinality of the set in question.*

Let me introduce terminology I will use in this thesis [18].

**Subgraph:** A subgraph  $G_s(V_s, E_s)$  of a graph  $G = (V, E)$  is a graph, where  $E_s \subseteq E$  and  $V_s = \{u, v : (u, v) \in E_s\}$ .

**Path:** A path is a non-empty graph  $P = (V, E)$  of the form

$$V = u_0, u_1, \dots, u_k \quad E = u_0u_1, u_1u_2, \dots, u_{k-1}u_k,$$

where the  $u_i$  are all distinct. The vertices  $u_0$  and  $u_k$  are linked by  $P$  and are called its ends. The number of edges of a path is its length.

**Node separation:** Node separation is the average of the length of the shortest path among all pair of nodes:

$$\ell = \frac{\sum_{v,u \in V} \min(M_P | P = (V_P = \{u, \dots, v\}, E_P))}{\binom{N}{2}}. \quad (2.1)$$

As the networks we have to deal with are usually of high order, we use also approximative algorithm with a random sampling technique to determine the node separation [63].

**Complete graph:** The graph is called *complete* if every pair of nodes is connected by an edge. The number of edges in a complete graph is

$$M_{complete} = \binom{N}{2}, \quad (2.2)$$

where  $N$  is the number of nodes.

**Connected component:** A connected component is the maximal subgraph where for every pair of nodes in the component there is a path connecting them.

**Directed and undirected graphs:** A graph is *directed* if the edge set contains ordered pairs of nodes. In other words a pair  $(u, v)$  means that there is an edge from the node  $u$  to the node  $v$  but no edge from  $v$  to  $u$ . When all edges in the graph are *undirected*, then also the graph is *undirected*.

**Node degree:** The *node degree*  $k_v$  of the node  $v$  is a number of edges incident with the node  $v$ . For directed graphs out-degree  $k_{out}$  (in-degree  $k_{in}$ ) denoting the number of edges pointing from (towards) the node is defined. Average node degree of a graph is determined as

$$\bar{k} = \frac{\sum_{v \in V} k_v}{N} = \frac{2M}{N}. \quad (2.3)$$

**Neighbourhood:** Denoted as  $\Gamma(v)$ , the *neighbourhood* of vertex  $v$  is the subgraph that consists of vertices adjacent to  $v$ , not including  $v$  itself.

**Clustering coefficient:** Clustering coefficient is defined as the ratio of edges existing in the neighbourhood of node  $v$  and number of edges which exists in  $\Gamma(v)$  if  $\Gamma(v)$  is a complete graph. The clustering coefficient  $c_v$  of a node  $v$  is defined as

$$c_v = \frac{|E(\Gamma(v))|}{\binom{k_v}{2}}. \quad (2.4)$$

Average clustering coefficient  $\bar{c}$  of a graph is simply an average of node clustering coefficients

$$\bar{c} = \frac{\sum_{v \in V} c_v}{N}. \quad (2.5)$$

## 2.2 Statistical properties of complex networks

Real networks have been intensively studied in last ten years [6, 10, 15, 46, 16]. They are usually characterized by several statistical properties such as:

**Degree distribution:** Degree distribution is a stationary function  $p(k)$  representing the probability that a node in a graph has the degree  $k$  [3].

$$p(k) = \frac{\sum_{v \in V} \delta(k - k_v)}{N}. \quad (2.6)$$

**Clustering distribution** Distribution of the average clustering coefficients of nodes with the degree  $k$ :

$$c(k) = \frac{\sum_{v \in V} \delta(k - k_v) c_v}{k}. \quad (2.7)$$

**Small world:** Surprisingly real networks possess many common properties. All such networks as the Internet [4], social networks[10], language networks [15], functional brain networks[16] or phone call networks [1] have a structure combining high clustering coefficient (2.5) with a low separation of nodes. These networks are called *small world* networks. This term was for the first time used by the Hungarian writer Frigyes Karinthy in 1929 [35]. He speculated that anyone in the world could be connected to anyone else through a chain consisting of no more than six intermediaries. This hypothesis was verified by Stanley Milgram [44] in his famous Milgram experiment. To express the small world-ness of a network in one parameter, Humphries et al. [34] introduced a small-world index measure as:

$$si = (\bar{c}/\bar{c}_{random})/(\ell/\ell_{random}), \quad (2.8)$$

where  $\bar{c}$  is the average clustering coefficient of the candidate network and  $\bar{c}_{random}$  is the average clustering coefficient of a random graph with the same size. Characteristics  $\ell$  and  $\ell_{random}$  then denote the node separation of these networks. This small-world index should be  $> 1$  for any small world network [34]

**Scale-free:** It was discovered that many real networks have a decaying power law degree distribution [27]. For this networks,  $p(k)$  (2.6) can be expressed as

$$p(k) \propto k^{-\gamma} \quad (2.9)$$

where  $\gamma$  is a power law exponent.

If the power law degree distribution is a property of real networks, question arises about the natural creation of such networks. To explain how dynamics influences network structure, Barabási proposed a model which leads to networks with a power law degree distribution. He reveals: "The power law distribution thus forces us to abandon the idea of a scale, or a characteristic node. In a continuous hierarchy there is no single node which we could pick out and claim to be characteristic of all the nodes. There is no intrinsic scale in these networks. This is the reason my research group started to describe networks with power law degree distribution as *scale-free*" [4].

As a result of power law degree distributions, scale free networks have many nodes with a much higher degree than average. These well-connected nodes are

called *hubs* and play an important role in the network connectedness (*Fig. 2.1*) Albert and Barabási [5] have shown that scale-free networks are highly resistant to random node attacks. It means that one can remove many randomly selected nodes and will not harm the connectivity of the network. This makes them more attractive from the point of view of informatics and signal spreading in networks. However, under a targeted attack by removing just a few important well-connected hubs, the network becomes soon disconnected.

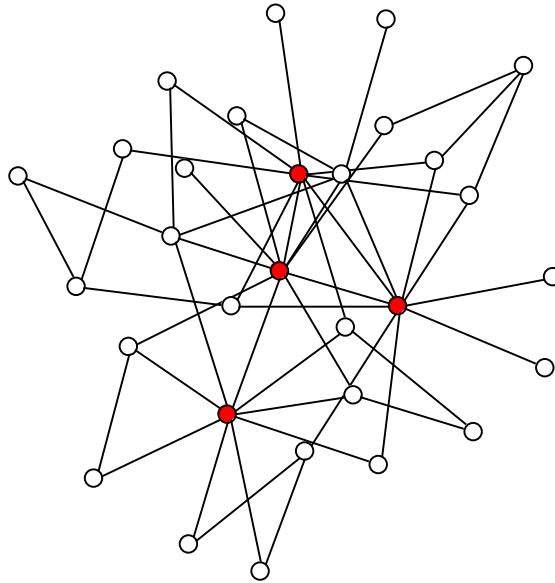


Figure 2.1: Structure of scale-free network. Well-connected nodes - *hubs* are highlighted. Scale-free network are highly resistant to random node attack. There are only few *hubs* that are critical for the connectedness of the network. However, it is enough to remove these nodes for a targeted attack to destroy the network structure.

The scaling exponent of the power law tail can be estimated from the histogram. If we make a logarithm of both sides of the power law distribution equation (2.9), we get  $\ln(p(k)) \approx -\gamma \ln(k)$ , which implies that the histogram of degrees follows a line in the log-log scale.

**Hierarchical topology:** Many networks are fundamentally modular: one can easily identify groups of nodes that are highly interconnected with each other, but have only a few or no links to nodes outside of the group to which they belong to [51]. These groups can represent friends, co-workers or communities. This modular organization is responsible for the high clustering coefficient that can be found in many real networks. These networks have clearly hierarchical structure. Ravász argues that this hierarchicity can be captured in a quantitative manner using a scaling law for the clustering distribution [51]. In hierarchical

networks clustering distribution  $c(k)$  (2.7) has the power law character

$$c(k) \approx k^{-\delta}, \quad (2.10)$$

which was also verified on several real-world networks[52, 50].

## 2.3 Network models

In this subsection I describe several well known models. This subsection has aim to show the state of the art in the theory and model construction of complex networks. Network features are very useful and there could be a desire to create networks with such properties. It would be nice to have a power grid networks resistant to random failures of transmitting nodes or computer networks with short path between routers. Hence there has been a lot of work on network generating models in parallel to the empirical studies of large real-world structures. Thanks to these models we can understand how dynamics influences the network structure and we can predict the statistical properties of the generated networks without long generation and computing. These models incorporate local (related to the node and its neighbourhood) or global (related to the whole network) rules or mechanism in a way that leads to the creation of a network with desired characteristics.

### 2.3.1 Random network

First attempts to model the structure of real networks were done using random graph models of Erdős and Rényi [26]. Erdős and Rényi introduced two equivalent random graph models (ER-model). One of them consists of  $N$  nodes and  $m$  edges chosen randomly from  $\frac{N(N-1)}{2}$  possible edges -  $G_{N,m}$  model. The other model is the binomial  $G_{N,\pi}$  model. Here we start with  $N$  nodes. Every pair will be connected with probability  $\pi$ , getting the total number of edges  $M_{G_{N,\pi}} = \pi \binom{N}{2}$ .

The greatest discovery of Erdős and Rényi was that many important properties of random graphs appear quite suddenly. That is, at a certain probability, either almost every graph has the property  $Q$ , or on the contrary, almost no graph has it. The transition from a property being very unlikely to being very likely occurs at critical probability  $\pi_c(N)$ . If  $\pi N$  grows slower than  $\pi_c N$  as  $N \rightarrow \infty$ , then almost every graph with connection probability  $\pi$  fails to have  $Q$ . If  $\pi N$  grows somewhat faster than  $\pi_c N$ , then almost every graph has the property  $Q$  [26].

Degree distribution of random graphs was studied by Béla Bollobás [13]. In a random graph with a connection probability  $p$ , the degree distribution is a binomial distribution

$$p(k) = \binom{N-1}{k} \pi^k (1-\pi)^{N-1-k}. \quad (2.11)$$

Actually, for large  $N$ , the binomial distribution follows the Poisson distribution

$$p(k) \simeq \frac{(N\pi)^k e^{-N\pi}}{k!}. \quad (2.12)$$

Random graphs tends to be spreading. With large probability the number of nodes at distance  $l$  from a given node is not much smaller than  $\bar{k}^l$ . Thus the node separation of random graph is [17, 3]

$$\ell_{random} = \frac{\log(N)}{\log(\bar{k})}. \quad (2.13)$$

In random graphs, the probability that two neighbours of any node are connected is equal to the probability that two randomly selected nodes are connected. Then we get that the clustering coefficient (2.5) of a random graph is [3]:

$$c_{random} = p = \frac{\bar{k}}{N}, \quad (2.14)$$

where  $\bar{k}$  is an average node degree and  $N$  the number of nodes. One can easily see that the clustering coefficient of a random network depends on its size, which is not true for real networks [3].

Random graphs are well known and there is a rich mathematical theory for the ER models. However, these models are generally insufficient to describe the structure of real networks.

### 2.3.2 Small world - Watts-Strogatz model

In their popular paper [64], Watts and Strogatz proposed a simple model (WS model) of a *small world* network. In this model a perfect ring structure turns into a random graph, by manipulating a single parameter [63]. The algorithm of small world network creation starts with a perfect 1d-lattice, in which each vertex has precisely  $k$  neighbours. It randomly rewires every edge of the lattice, with the probability  $p$ . The schematic picture is in (Fig. 2.2), and the process is algorithmised as follows:

1. Each vertex  $i$  is chosen in turn, along the edge that connects it to its nearest neighbour in a clockwise sense ( $i, i + 1$ ).
2. A uniform random number  $r$  is generated. If  $r \geq p$ , then the edge ( $i, i + 1$ ) is unaltered. If  $r \leq p$ , then ( $i, i + 1$ ) is rewired and vertex  $i$  is connected to another randomly chosen vertex  $j'$ .
3. When all vertices have been considered once, the procedure is repeated for edges that connect each vertex to its next nearest neighbour (that is  $i + 2$ ), and so on. In total  $k/2$  such rounds are completed, until all edges in the graph have been considered for rewiring.

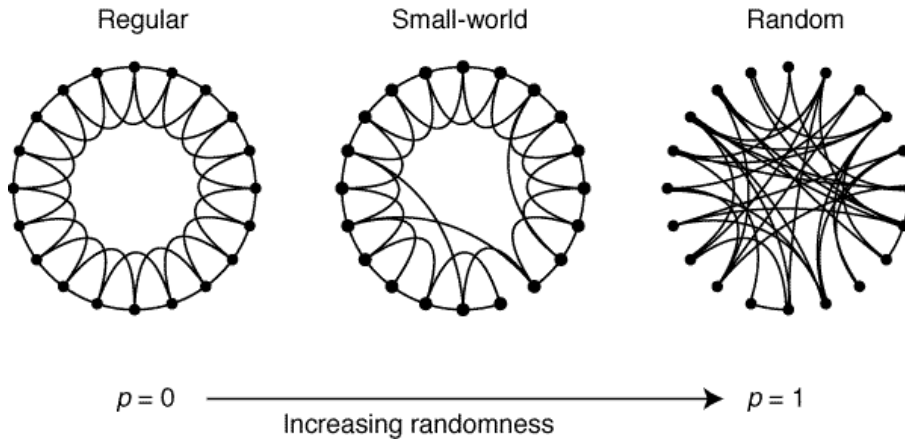


Figure 2.2: Evolution of network with the WS model construction algorithm for  $k = 4$ . For  $p = 0$ , the original 1-lattice structure remains, for  $p = 1$ , all edges are rewired randomly [64].

The greater is the rewiring probability, the more shortcuts between distant nodes are created. This leads to a fast drop of the node separation  $\ell(p)$  already for small values of the parameter  $p$ . On the other hand, clustering coefficient remains high and drops down for  $p \rightarrow 1$  (Fig. 2.3). Thus if we want to generate small world networks which are known to have small  $\ell$  and large clustering coefficient, we have to use parameter  $p$  between 0 and 1 [63].

### 2.3.3 Preferential attachment - Barabási-Albert model

Because random graph models were insufficient to explain the structure of real networks, there were attempts to find better models. The most successful one is a model suggested by Barabási and Albert. They introduced the idea of preferential attachment as a natural process of network development [9]. Barabási-Albert model (BA model) grows in time. Nodes are arriving one at the time. When a new node arrives it links itself by  $m$  edges to some old nodes ( $m$  is a constant parameter). The old nodes are not chosen at random but with some preference. In the BA model the preference is proportional to an old node degree. The algorithm as proposed by Barabási and Albert is:

1. Start with a small number ( $N_0$ ) of randomly connected nodes.
2. Every time step add a new node and connect it by  $m$  edges to nodes already present in the graph. These  $m$  nodes are chosen preferentially that means that the probability  $\Pi$  that a new vertex will be connected to vertex  $i$  depends on the degree  $k_i$  of that vertex

$$\Pi(k_i) = \frac{k_i^m}{\sum_{i=1}^{N-1} k_i^m}. \quad (2.15)$$

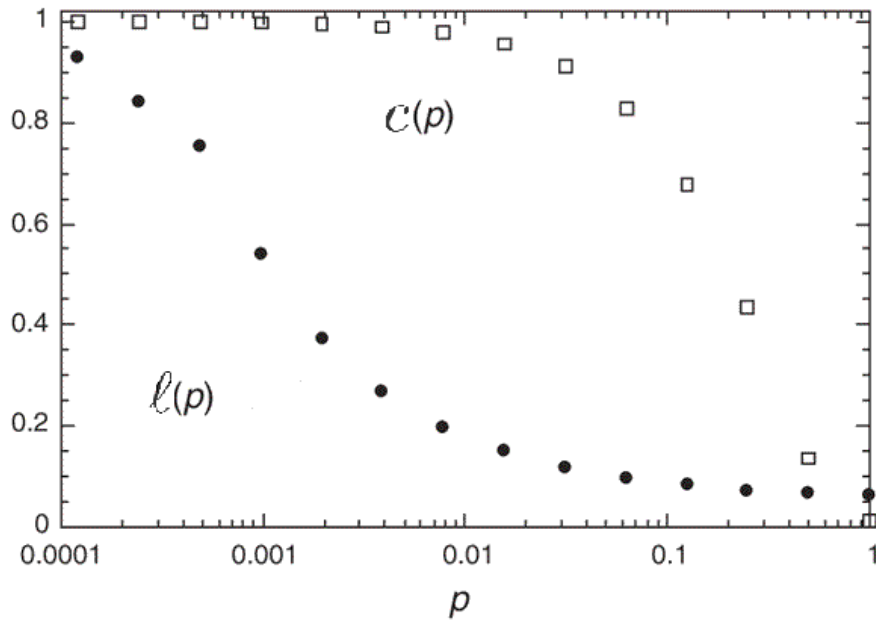


Figure 2.3: Node separation  $\ell(p)$  and clustering coefficient  $c(p)$  for the WS model. Empirical studies of the networks generated via the WS model has shown that the node separation  $\ell(p)$  drops from the  $L_{1-lattice} = \frac{n(n+k-2)}{2k(n-1)}$  down to size of  $\ell_{random}$  (2.13) very soon and remains there until  $p = 1$ . The clustering coefficient starts at the size of  $c_{1-lattice} = \frac{3}{4} \frac{(k-2)}{(k-1)}$ , remains relatively high and drops down to the small size comparable to that of clustering coefficient of random graphs  $c_{random}$  (2.14) when  $p \rightarrow 1$ . [64]

This process leads to the network with a power law degree distribution with the coefficient  $\gamma = 3$  (Fig. 2.4). This can be also proven through the analytical solution proposed by Barabási and Albert [22]. Their solution uses an idea of continuous approach, which assumes that for large networks the  $k_i$  is a continuous variable and thus the BA process can be described by the differential equation

$$\frac{\partial k_i}{\partial t} = m\Pi(k_i) = m \frac{k_i}{\sum_{j=1}^{N-1} k_j}. \quad (2.16)$$

It is easy to see, that the sum in denominator is  $\sum_{j=1}^{n-1} k_j = 2mt - m$ . Using the initial condition that every node at its introduction time  $s_i$  has  $k_i(s_i) = m$  edges, we get the solution

$$k_i(t) = m \left( \frac{t}{s_i} \right)^\beta, \quad \text{with } \beta = \frac{1}{2}. \quad (2.17)$$

With a help of the equation (2.17), the probability that a node degree  $k_i(t)$  is lower than  $k$ , can be written as [3]

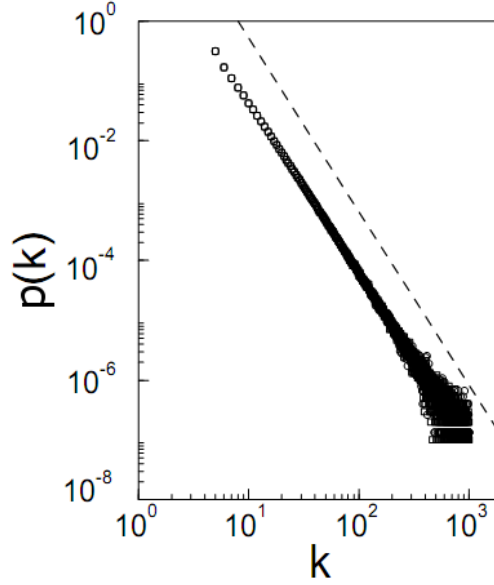


Figure 2.4: The power law degree distribution at  $t = 150000$  obtained from the BA model, using  $m_0 = m = 5$ . The slope of the dashed line is  $\gamma = 3$ . The plot is made in the log-log scale. [9]

$$P(k_i(t) < k) = P(s_i > \frac{m^{1/\beta}t}{k^{1/\beta}}). \quad (2.18)$$

If we assume that we add all nodes at equal intervals, the probability density of  $s_i$  is constant ( $p(s_i) = \frac{1}{N_0+t}$ ). Substituting this to (2.18), the equation for the stationary degree distribution reads

$$p(k) = \frac{\partial P(k_i(t) < k)}{\partial k} = \frac{2m^{1/\beta}t}{N_0+t} \frac{1}{k^{1/\beta+1}}. \quad (2.19)$$

For  $t \rightarrow \infty$  solution of (2.19) is [3]:

$$p(k) \sim 2m^{1/\beta}k^{-\gamma_{BA}}, \quad \text{with } \beta = \frac{1}{2} \quad \gamma_{BA} = \frac{1}{\beta} + 1 = 3. \quad (2.20)$$

There is another possible analytical treatment of the BA model introduced by Dorogovtsev and Mendés [24]. It is the *master equation approach*: Whenever in the BA process a new node is added, the degree of an old node  $i$  increases with the probability  $m\Pi(k) = k/2t$ , with the probability  $1 - k/2t$  it stays the same. The process is described by the master equation

$$P(k, s, t+1) = \frac{k-1+m}{2t}P(k-1, s, t) + \left(1 - \frac{k+m}{2t}\right)P(k, s, t), \quad (2.21)$$

where  $P(k, s, t)$  means the probability that at time  $t$  the node introduced at time  $s$  has a degree  $k$ . Having the probability  $P(k, s, t)$ , the degree distribution can be expressed as

$$p(k) = \lim_{t \rightarrow \infty} \left( \sum_s P(k, s, t) \right) / t. \quad (2.22)$$

Applying  $\sum_{s=0}^t$  and (2.22) to (2.21) and passing to the  $t \rightarrow \infty$  limit, one gets

$$p(k) + \frac{1}{2} [(k+m)p(k) - (k-1+m)p(k-1)] = \delta_{k,1}. \quad (2.23)$$

In the continuous  $k$  limit, this equation has a form

$$p(k) + \frac{1}{2} \frac{\partial [(k+m)p(k)]}{\partial (k+m)} = 0, \quad (2.24)$$

which leads to the solution [22]

$$p(k) = \frac{2m(m+1)}{(k+m)(k+m+1)(k+m+2)}, \quad (2.25)$$

what for large  $k$  gives (2.20).

### 2.3.4 Accelerated growth - Dorogovtsev-Mendés model

Interesting modification of the model of Barabási and Albert was introduced by Dorogovtsev and Mendés (DM model)[21]. Authors have combined the idea of preferential linking [9] with the idea of accelerated growth [21]. Supported by empirical observations, in many networks, number of edges grows much faster than the number of nodes. This means that there are edges created also between the nodes already present in the network. This is called *acceleration*. The idea of accelerated growth in general is as follows. In each step, in addition to the nodes attachment as in the BA model (Section 2.3.3) new edges are added between old nodes. This is included in the DM growing network:

1. Start with a small number ( $N_0$ ) of randomly connected nodes.
2. Every time step add a new node with  $m$  edges that connect this node preferentially to the old nodes (2.15).
3. In the same time create other  $ct$  edges and link them to the old nodes preferentially.  $c$  is a small constant ( $c \ll 1$ ).

Using a continuous approach [22], the change of the node degree in this model can be described by following equation:

$$\frac{\partial k(s, t)}{\partial t} = (m + 2ct) \frac{k(s, t)}{\int_0^t du k(u, t)}, \quad \text{with } k(t, t) = m, \quad (2.26)$$

where  $k(s, t)$  is an average degree of a node born at the time  $s$  and observer at the time  $t$ . In this particular model it is easy to see, that

$$\int_0^t du k(u, t) = 2mt + ct^2. \quad (2.27)$$

Therefore the average degree is:

$$\bar{k} = 2m + ct. \quad (2.28)$$

The solution of (2.26) using (2.27) is

$$k(s, t) = m \left( \frac{ct}{cs} \right)^{1/2} \left( \frac{2 + ct}{2 + cs} \right)^{3/2}. \quad (2.29)$$

To obtain the degree distribution  $p(k)$  we need to solve the equation  $p(k, t) = -[t\partial k(s, t)/\partial s]^{-1}$  [20]. The solution is

$$p(k, t) = \frac{1}{ct} \frac{cs(2 + cs)}{1 + 2cs} \frac{1}{k}. \quad (2.30)$$

One can see in (2.29) that  $k(s, t)$  scales like  $\propto s^{-\frac{1}{2}}s^{-\frac{3}{2}}$ . If  $k$  scales like  $s^{-\beta}$ , degree distribution  $p(k)$  gives us the power law distribution  $k^{-\gamma}$ , where  $\gamma = 1 + 1/\beta$ . This gives us two distinct regimes for DM model (Fig. 2.5). The crossover point is  $k_{cross} \approx \sqrt{ct}(2 + ct)^{3/2}$  [20]. Below this crosspoint  $\gamma_{DM} = 3/2$ . Over the crosspoint  $\gamma_B A = 3$ .

This model was used by Dorogovtsev and Mendéz to explain two power law regimes in the degree distribution of the word web [20].

### 2.3.5 Exponential tail

It is known, that several networks show deviations from the power law degree distribution. In some networks such as actor networks [10] or those of functional brain networks [2] degree distribution has an exponential tail for large  $k$ . The question is: what is the reason for such a decay? Common feature of these networks are constraints limiting the addition of new edges. For example the actor networks represent a type of network with the aging of nodes. In this network nodes are actors. An edge is present if two actors are performing together in a movie or play. One day, every actor will stop acting. From this time, the node representing this actor will stop receiving new links, even if it is a highly connected node. The aging of nodes thus affects the degree distribution of the network. Network of neurons in our brain is an example of a network with a limited capacity of nodes. There are physical boundaries for the number of connections one neuron can have. When a neuron reaches this number of connections, it will stop receiving new connections.

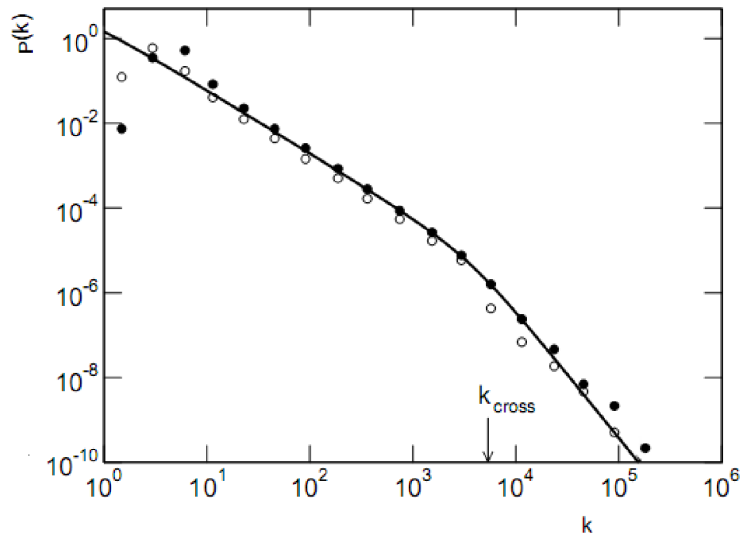


Figure 2.5: Log-log plot of the degree distribution for the DM model with accelerated growth, with the parameters  $t \approx 470,000$  and  $\bar{k} \approx 72$ . Two different scaling regimes with exponents  $3/2$  and  $3$  are seen, together with the  $k_{cross}$  point [20]

Aging of nodes in network models was introduced by Amaral et. al [7]. The idea is following. If a node reaches a certain age or the cost of the node capacity which is a defined threshold, new edges cannot connect to it. Sometimes a cost function of adding a new edge to a node, proportional to its capacity is used to restrict the node degree growth. Numerical results (*Fig.2.6*) show that both types of constraint lead to cutoffs of the power law decay of the tail of degree distribution.

The presence of exponential tail was reported in many scale-free networks, but not as a result of aging but simply as a finite size effect. This effect is captured by the following equation:

$$P(k, t) \propto k^{-\gamma} e^{-\frac{k}{k_{cutoff}}}, \quad (2.31)$$

where  $k_{cutoff}$  is the point where the distribution changes from the power law which scales over the finite region before the cutoff point to the exponential tail [7].

### 2.3.6 Hierarchical network model

I have already mentioned that some structural properties are similar in several real networks. Many real networks combine scale-free structure with a hierarchical organization of nodes. BA model shows how the scale-free structure emerges, but

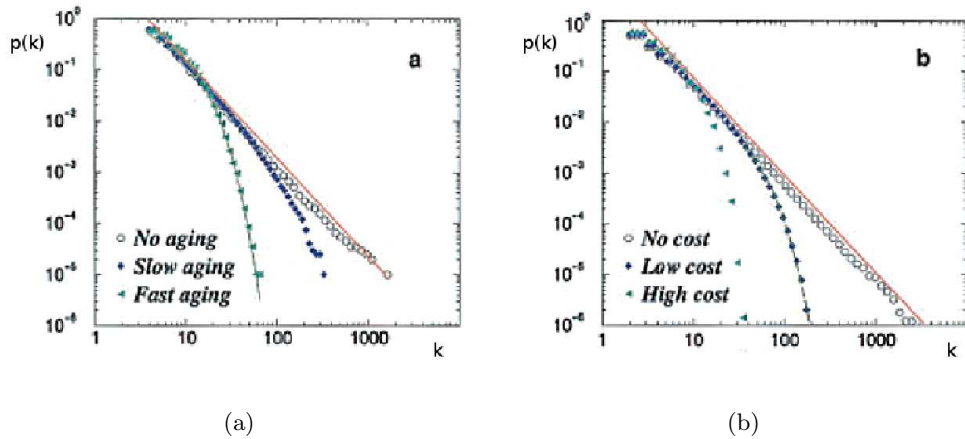


Figure 2.6: Truncation of scale-free connectivity by adding constraints to the BA model. (a) Effect of aging of vertices on the connectivity distribution. We see that aging leads to a cutoff of the power law regime in the connectivity distribution. (b) Effect of cost (capacity) of adding links on the connectivity distribution. These results indicate that the cost of adding links also leads to a cutoff of the power law regime in the connectivity distribution. Both plots are in log-log scale [7].

does not explain the hierarchy. Hierarchy in networks was studied by Ravász and Barabási [51]. They introduced a network growing process (RB model) leading to a hierarchical scale-free network

1. Start from a complete graph of 5 nodes (*Fig. 2.7 – a*).
2. In each step generate four replicas of the existing graph and connect the external nodes of the replicas to the central node of the initial module (*Fig. 2.7 – b – c*).

Numerical simulations indicate that RB model leads to a network with a power law degree distribution with the exponent  $\gamma = 1 + \ln(5)/\ln(4) = 2.161$  and that the clustering coefficient  $\bar{c} \simeq 0.743$  is independent of the size of the network (*Fig. 2.8 – a – c*). Hierarchical structure is revealed in the power law clustering distribution (2.7). The nodes at the center of the numerous five-node modules have the clustering coefficient  $c_5 = 1$ . Those at the center of a 25-node module have  $k = 20$  and  $c_{25} = 3/19$ , while those at the center of the 125-node modules have  $k = 84$  and  $c_{125} = 3/83$ . Thus nodes with a higher node have smaller clustering coefficient asymptotically following  $c(k) \approx k^{-1}$  (*Fig. 2.8 – b*).

RB model has one significant disadvantage. It is too deterministic to be a model of real network. Another question is: is the power law clustering distribution (2.10) valid for all networks with hierarchy, or the  $\delta$  exponent can change?

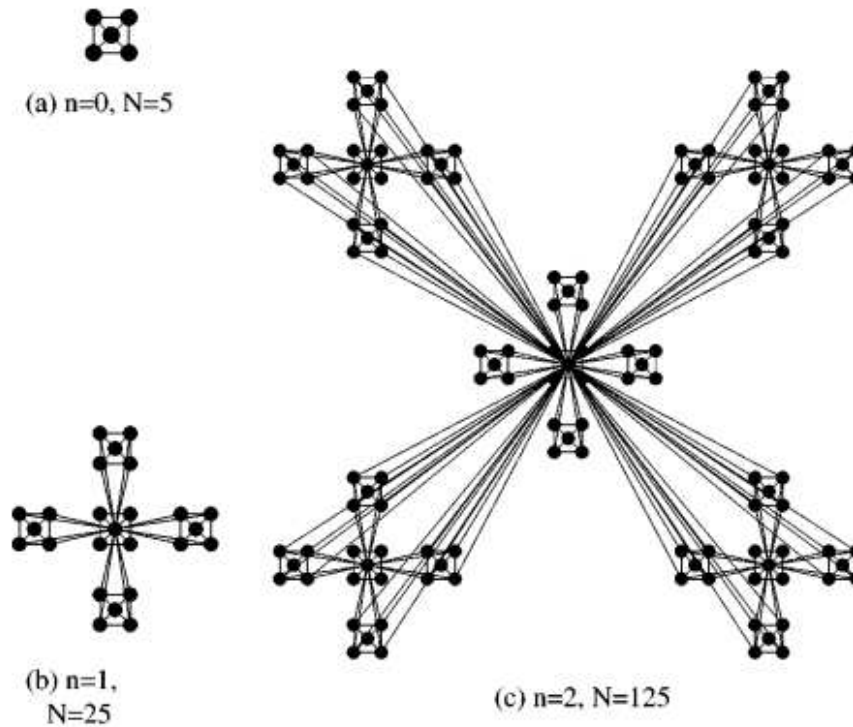


Figure 2.7: The iterative construction leading to a hierarchical network. Starting from a fully connected graph of five nodes shown in (a), four identical replicas are created. Peripheral nodes of each new module are connected to the central node of the initial module, obtaining a network of  $N = 25$  nodes (b). In the next step, we create four replicas of the 25 node module, and connect the peripheral nodes again, as shown in (c), to the central node of the initial module, obtaining a  $N = 125$ -node network. This process continues further [51].

To make their model more realistic, Ravász and Barabási proposed a stochastic model [51]. They modified the RB process. In each step, only a  $p^i$  fraction of new nodes is connected to the central node. Remaining new nodes are connected to the old nodes preferentially.  $i$  denotes the  $i$ -th iteration of the algorithm. In this process, increasing  $p$  decreases the exponents  $\gamma$  and  $\delta$ . The presence of such a hierarchical architecture reinterprets the role of hubs in complex networks. With a decreasing clustering coefficient, hubs have a small chance of linking to each other. Therefore, hubs play an important role of bridging many small communities of clusters into a single, integrated network [51].

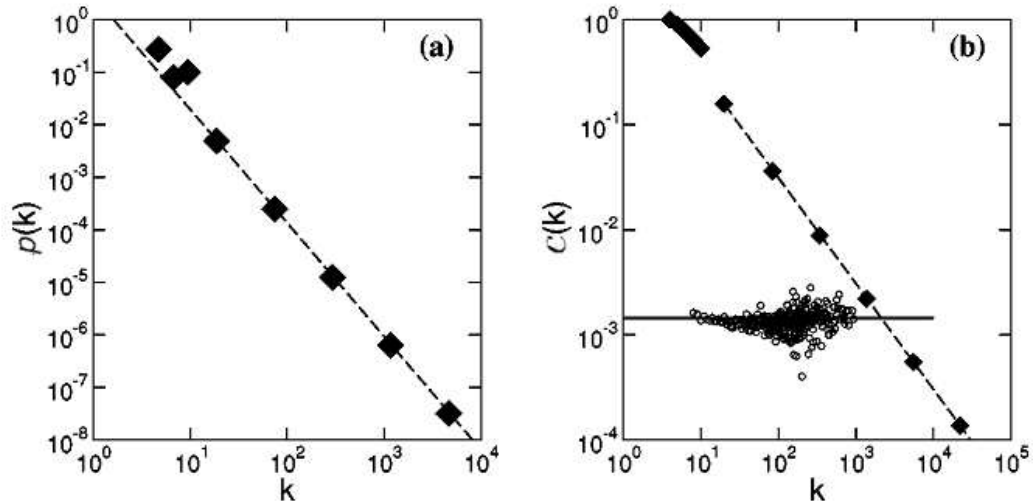


Figure 2.8: Scaling properties of the hierarchical model shown. (a) degree distribution. (b)  $c(k)$  curve for the model, demonstrating that it follows  $k^{-1}$ . The open circles show  $c(k)$  for a BA model of the same size, illustrating that it does not have a hierarchical architecture. [51]. All plots are in log-log scale.

### 2.3.7 Random walk model

Another interesting model of a complex network was introduced by Vázquez and inspired by modeling the WWW surfers as random walkers on a graph [62]. He claims that local rules are decisive to construct a hierarchy in growing networks. This model incorporates a different point of view: Is it possible to learn about the network structure by surfing? If the surfers explore WWW, they do that by two different processes: jumping randomly to a certain node or exploring the network by moving along edges (WWW-links). Surfers combine both of these possibilities. Moreover they also modify the network by adding a new link here and there. Assume that we have a network but we do not know its structure. A surfer starts with a randomly chosen node. Then with the probability  $q_e$  he decides to follow one edge adjacent to that node or jump to another random node with the probability  $1 - q_e$ . Thus surfer reveals the network structure. Each time he visits a new node this node is "added" to the network. When visiting a node surfer can create a new edge to it with a probability  $q_v$ .

Let us denote  $v_i$  the probability that a vertex  $i$  will be visited and  $q_v$  the probability that a visited vertex increases its degree by 1 (an edge is connected to it). The probability  $v_i$  can be expressed as

$$v_i = \frac{1 - q_e}{N} + q_e \Theta k_i, \quad (2.32)$$

where

$$\Theta = \frac{\bar{v}}{\bar{k}} \quad (2.33)$$

is the average probability that a vertex pointing to vertex  $i$  is visited and  $k_i$  is the vertex degree. The first term of (2.32) describes a probability of random jump to a network node, the other one is the probability that the surfer comes to the node  $i$  from certain neighbour. During a walk  $\bar{v}N$  vertices are visited, adding  $q_v\bar{v}N$  edges on average. Using this we have

$$\frac{\partial N}{\partial t} = v_a, \quad (2.34)$$

$$\frac{\partial M}{\partial t} = v_s q_v \bar{v} N, \quad (2.35)$$

where  $M$  is the number of edges, and  $v_s$  and  $v_a$  are the number of surfers and the number of newly added nodes per unit time, respectively [62]. From equations (2.33), (2.34), (2.35) we have

$$\Theta = \frac{v_a}{q_v v_s \bar{v} N}. \quad (2.36)$$

Using equations (2.32) and (2.36) we can express the probability that the degree of a vertex of degree  $k$  increases by 1 when a surfer walks on the graph as

$$A_k = \frac{1}{N} \left[ q_v (1 - q_e) + q_e \frac{v_a}{v_s} k \right]. \quad (2.37)$$

To find the degree distribution of the network, we have to find the number of vertices  $n_k$  with the degree  $k$  that satisfies the rate equation [23, 62]

$$\frac{\partial n_k}{\partial t} = v_s A_{k-1} n_{k-1} - v_s A_k n_k + v_a \delta_{k,0}. \quad (2.38)$$

For the networks with a constant growth rate, which satisfies the condition that  $v_s/v_a$  is constant, the degree distribution reaches a stationary state and we can write

$$n_k(t) = N p(k), \quad (2.39)$$

where  $p(k)$  is the stationary probability that a vertex has the degree  $k$  [62]. Substituting this expression in (2.38), we obtain that the asymptotic behavior for large  $k$  is

$$p(k) = \frac{1}{1+a} \frac{\Gamma[a(\gamma-1)+k]}{\Gamma[a(\gamma-1)]} \frac{\Gamma[(1+a)(\gamma-1)+1]}{\Gamma[(1+a)(\gamma-1)+k+1]}, \quad (2.40)$$

where

$$\gamma = 1 + \frac{1}{q_e}, \quad a = \frac{v_s}{v_a} q_v (1 - q_e) \quad (2.41)$$

and  $\Gamma$  denotes the *Gamma*-function.

To get (2.40) I and my co workers found another approach [48]. Using the fact that  $p(k)$  is stationary distribution and including (2.39) in (2.38) we have

$$\frac{\partial Np(k)}{\partial t} = -v_s [A_k Np(k) - A_{k-1} Np(k-1)] + v_a \delta_{k,0}. \quad (2.42)$$

For large  $k$  it is possible to take  $k$  as a continuous variable [22] and take the change from  $k-1$  to  $k$  as small. With a help of (2.34) and (2.37) one can rewrite the equation (2.42):

$$\frac{\partial Np(k)}{\partial t} = -\frac{\partial A_k Nv_s p(k)}{\partial k}, \quad (2.43)$$

$$v_a p(k) = -v_s \frac{\partial \left[ q_v(1 - q_e)p(k) + q_e \frac{v_a}{v_s} k p(k) \right]}{\partial k} \quad (2.44)$$

$$\frac{\partial p(k)}{p(k)} = \frac{v_a(1 + q_e)\partial k}{(q_e - 1)v_s - q_e v_a k}. \quad (2.45)$$

This leads to the solution

$$p(k) \propto k^{-\gamma}, \quad \gamma = 1 + \frac{1}{q_e} \quad (2.46)$$

The solution is in a perfect agreement with Vázquez [62]

Hence we can see that the random walk model leads to the power law degree distribution showing the scale-free structure of the explored part of the network. Vázquez[62] provides also analytical evidence that clustering distribution of the explored network scales as

$$c(k) \approx \frac{2(1 + q_e)}{k} \approx k^{-1}. \quad (2.47)$$

This indicates that this model creates hierarchical network.

To explore all of the models describing complex networks is beyond the scope of this work. I chose to present a deeper intrigue only to those models, which are decisive for my own studies. In the next chapters I am presenting my own results on positional word web, network hierarchy and functional brain networks. This work has been done in cooperation with my co-workers Mária Markošová, Ľubica Benušková and Boris Rudolf.

## Chapter 3

---

# Positional word web

---

### 3.1 Introduction

Word webs have been studied by Cancho and Solé [15], Dorogovtsev and Mendés [20] and Markošová [40]. In the positional word web nodes are words and edge is added if two words are neighbours in a sentence. Cancho and Solé studied positional word web created from texts in the English national corpus (CS word web) [15]. The authors have shown, that the degree distribution indicates preferential addition of nodes. But there are two different scaling regimes, one for well connected kernel lexicon words and the other for less connected ones. By kernel lexicon we understand the basic set of words common for all people using the same language. They guess, that the kernel vocabulary has different dynamics, than the non kernel one.

The results of Cancho and Solé were revised by Dorogovtsev and Mendés and by us [20, 40]. Markošová [40] proposes a model which gives possible explanation of the difference between measured data and the explanation of two scaling regimes given by Dorogovtsev and Mendés. [20]. This model extends the DM model (2.3.4) with a rewiring of existing edges. I made detailed studies of the proposed model, and a numerical and analytical one as well. I have created a word web of the ancient text, The Bible, which did not change its vocabulary for several hundreds of years. I have used The Bible positional word web (BWW) to test the proposed model. In this chapter I present results of these studies [47].

### 3.2 Word web

Lexicon of the human language is composed of hundred thousands of words. Let us have, for example the English language. English national corpus consists of about 500000 words [15]. Not all of them are used by all members of the

English population. There are words, which are frequent and understandable for everybody, independently of their age, education, etc. This set is called **kernel lexicon** and includes about ten thousand words.

What is the structure of the lexicon and how is it implemented in our brain? By structure I do not mean the correspondence with the anatomical brain networks, but simply how the word is used. How one word leads to the retrieval of accustomed lexical structures. For example, how is it used in sentences? This is a good question, if we have in mind, how great the word database is and how quickly our brain retrieves in it. Several studies have been made to find the answer [15, 46, 63]. All of them shows, that the structure of positional word web is scale free and small world like.

As I have already mentioned in Sections 2.2 and 3.1, degree distribution of the positional word web indicates scale free structure (2.9), but with two different scaling regimes [20]. For well-connected words with great degree, the scaling exponent  $\gamma_{DM}^2$  is close to  $\gamma_{BA} = 3$ . Less connected words scale with  $\gamma_{DM}^1 = 1.5$ . Empirical results of Cancho and Solé [15] were explained by the model of Dorogovtsev and Mendés [20] (2.29).

Dorogovtsev and Mendés do not agree, that the different scaling means different dynamics in kernel and non kernel vocabulary. They rather reason, that the two scaling regimes occur due to some additional processes running together with the preferential node addition (see 2.3.4).

In addition to the well known Albert-Barábasi mode [9], the DM process includes the following process:

1. Start with a small number ( $N_0$ ) of randomly connected nodes.
2. Every time step add a new node with  $m$  edges that connect this node preferentially to the old nodes (2.15).
- 3. Simultaneously with addition of a new node with  $m$  edges, add  $ct$  new edges (that means  $2ct$  edge ends,  $c \ll 1$ ) unit and connect the old nodes with a preference.**

What all this means in the word web terminology? The new nodes are in fact new words which time to time appear in the vocabulary. They are included in the context of the old ones. But simultaneously, several old words (nodes) enrich their own meaning. They are used with some words, with which they have not been used before. Let us mention one example. To tell the sentence "Portable computer has a new design" in sixties had no sense. Word "computer" was not used together with "portable", because computers were big devices. Now it is quite OK.

As we already know (2.29), in the DM model  $k(s, t)$  scales with  $s$  as  $k(s, t) \propto s^{-\beta}$ . It has been shown, that scaling exponent  $\gamma$  of the degree distribution ( $p(k) = k^{-\gamma}$ ) is related to  $\beta$  as [21]

$$\gamma = 1 + \frac{1}{\beta}. \quad (3.1)$$

In the case of the DM model  $k(s, t) \propto s^{-\frac{1}{2}}s^{-\frac{3}{2}}$ . For  $s \ll t$  (well connected words)  $\beta_{DM} = \frac{1}{2}$  and  $\gamma_{DM}^2 = 3$ , and for  $s \sim t$  (less connected words)  $\beta_{DM} = \frac{1}{2} + \frac{3}{2}$  and  $\gamma_{DM}^1 = 1.5$  [20].

DM model therefore explains the two scaling regimes in the degree distribution of the CS word web. But, as it has been measured by Cancho and Solé [15], the scaling exponent of the steeper part of the real word web is not  $\gamma_{BA} = 3$ , but somewhat lower ( $\gamma = 2.7$ ). The difference between measured and theoretical values indicates, that there might be other processes, not included in the DM model, which influence the distribution [40].

### 3.3 Word web model

What are the other processes, which should be considered? Let us reason a little. New words are created and added to the vocabulary all the time, of course. But not only this. The meanings of old words also develop in time. Some of them appear in a new context. Sometimes they lose some of their previous meanings, and get another.

In the network terminology the addition of a new context means the appearance of new edges between old words. This has been encountered in the DM model, leading to the two different scaling regimes. Losing a meaning and getting a new one means, that some ends of old edges are rewired. Edge rewiring can be preferential, random, or a combination of both.

To fit the measured data in the CS word web [15, 38] a minimal model inspired by the DM model and by [23] was suggested [40]. In this new model, these processes are included:

1. Start with a small number ( $N_0$ ) of randomly connected nodes.
2. Every time step add a new node with  $m$  edges that connect this node preferentially to the old nodes (2.15).
3. Simultaneously with addition of a new node with  $m$  edges, add  $ct$  new edges (that means  $2ct$  edge ends,  $c \ll 1$ ) unit and connect the old nodes with a preference.
4. **In the same time select randomly  $m_r$  old nodes and rewire one edge end of each of them preferentially.**

If these processes run a long time, continuum approach [23] is describing the average degree  $k(s, t)$  of node  $s$  in time  $t$ . In this approximation  $k(s, t)$  is a continuous variable. The dynamical equation describing above mentioned processes is as follows:

$$\frac{\partial k(s, t)}{\partial t} = (m + 2ct + m_r) \frac{k(s, t)}{\int_0^t k(s, t) ds} - \frac{m_r}{t} \quad (3.2)$$

The first addend in (3.2) defines preferential linking. The second one represents random selection of edge ends to be rewired. In the first addend the term  $m \frac{k(s, t)}{\int_0^t k(s, t) ds}$  represents preferential linking of  $m$  new edges,  $2ct \frac{k(s, t)}{\int_0^t k(s, t) ds}$  describes preferential linking of  $2ct$  new edge ends among old nodes and  $m_r \frac{k(s, t)}{\int_0^t k(s, t) ds}$  tells that  $m_r$  edge ends are rewired preferentially.

To solve this equation, the integral  $\int_0^t k(s, t) ds$ , giving the sum of all degrees in the net, needs to be specified. This sum is influenced only by the new link creation; rewiring left it unaffected. Because the only edge creation processes are the same as in the DM model, the integral is given by (2.27).

Substituting (2.27) into (3.2) the equation (3.2) is reformulated:

$$\frac{\partial k(s, t)}{\partial t} = (m + 2ct + m_r) \frac{k(s, t)}{2mt + ct^2} - \frac{m_r}{t} \quad (3.3)$$

This is a simple linear first order differential equation of the type

$$\frac{\partial y}{\partial x} = -f_1(x)y - f_2(x) \quad (3.4)$$

with the solution

$$y = e^{-\int f_1(x) dx} \left[ \phi - \int f_2 e^{\int f_1(x) dx} dx \right]. \quad (3.5)$$

Using (3.5) we get

$$k(s, t) = \left(\frac{t}{s}\right)^A \left(\frac{2m + ct}{2m + cs}\right)^{2-A} g(s, t) \quad (3.6)$$

where  $A = \frac{m+m_r}{2m}$  and

$$g(s, t) = \frac{1}{m^2 - m_r^2} \left( m + \frac{m_r}{m^2 - m_r^2} \left[ M_1 + M_2 \left(\frac{s}{t}\right)^A \left(\frac{2m + cs}{2m + ct}\right)^{2-A} \right] \right) \quad (3.7)$$

where  $M_1 = (2m + cs)(m - m_r + cs)$  and  $M_2 = (2m + ct)(m - m_r + ct)$ .

Then the leading term of (3.6) is  $\left(\frac{t}{s}\right)^{\frac{m+m_r}{2m}} \left(\frac{2m+ct}{2m+cs}\right)^{2-\frac{m+m_r}{2m}}$ . If  $m \neq m_r$ ,  $g(s, t)$

(3.7) doesn't influence the solution too much. From (3.6) it is clear, that

$$\text{-if } s \ll t, \beta = \frac{m+m_r}{2m} \text{ and } \gamma = 2 + \frac{m-m_r}{m+m_r},$$

-but if  $s \sim t$ ,  $\beta = 2 - \frac{m+m_r}{2m} + \frac{m+m_r}{2m} = 2$  and thus  $\gamma = 1.5$ .

In the model (3.2) scaling exponent  $\gamma$  is lower than the value  $\gamma_{BA} = 3$  in the region of great  $k$ , but maintains the value 1.5 in the region of small  $k$ -s. This is exactly what has been measured by Cancho and Solé [15]. DM model describes their data but the scaling of the degree distribution (2.6) is  $\gamma_{DM}^2 = \gamma_{BA} = 3$  in the steeper part. Additional effect of link rewiring included into the model removed this discrepancy.

### 3.4 Numerical studies of the word web

My goal was to test if the model (3.2) also fits the distribution of the real word web of a special kind. Namely, I wanted to know, whether the word web based on an ancient text, which has not changed for a long time, has the same two-modal scaling, as the web based on the modern English vocabulary. In restricted vocabulary of The Bible no new words are added in time and no words change their meaning or context.

To do this, I have created a positional word web on the basis of several versions of English translations of The Bible (BWW net) [12]. First the small world properties of each BWW net were measured. All parameters are collected in the Table 3.1. As shown, all word webs combine high clustering with small node separation, which is typical for the small world networks [63].

version	N	$\bar{c}$	$\ell$	$\bar{k}$
kjv	11592	0.771	2.18	47
drv	11379	0.772	2.18	47
asv	10077	0.778	2.18	47
nrsv	14717	0.718	2.24	50
bev	4942	0.774	2.12	70
prg	21104	0.700	2.27	49

Table 3.1: Properties of positional BWW. Here N is the number of distinct words in the text,  $\bar{c}$  is the BWW clustering coefficient,  $\ell$  denotes the node separation,  $\bar{k}$  the average node degree. We have used several versions of The Bible [12]. Some of them, such as King James version (kjv), Douay Rheims version (drv) are old (kjv has been issued in the year 1711, drv is even older, 1582), the others (American Standard version, asv, 1901; Basic English version, bev, 1941; New Revised Standard version, nrsv, 1989) are relatively modern. bev is special, because its text has been artificially simplified. It is reflected in slightly different parameters in the table. prg is the word web created from the selected books found in the Project Gutenberg web page [31]. This has been added for comparison of the parameters of the ancient and the modern text.

I have also generated artificial networks, programming the processes proposed in the previous Section (3.2). The parameters of the model were taken from the kjv and the prg word webs. In the experiment of Cancho and Solé [15], there are no multiple edges considered. The analytical equations (2.26, 3.2), however, do not exclude them.

To test the role of multiple edges, artificial networks (having  $N = 20000$  nodes) were developed, once with allowed and also disallowed multiple edges. Degree distributions of all networks (BWW, artificially created) are depicted on (Fig. 3.1), together with corresponding average scaling exponents. All of the networks have the power law degree distribution indicating scale free structure, but there are no two scaling regimes present.

The most probable reason of this discrepancy between the theory (3.2) and the data is, that our data sets are too small. In the DM model, there is a crossover point [20]

$$k_{cross} = m(ct)^{\frac{1}{2}}(2 + ct)^{\frac{3}{2}} \quad (3.8)$$

between the two scaling regimes. Calculating  $k_{cross}$  for generated networks with  $N = t = 20000$  nodes and kjv and prg parameters ( $m = 4, c = 0.003$  for kjv and  $0.002$  for prg,  $m_r = 2$ ) we get  $k_{cross}$  values out of the  $k$  - range of the degree distribution (Fig. 3.1). To test this hypothesis, I have decreased parameter  $c$  in (3.8) to get lower  $k_{cross}$ . Now, as seen on (Fig. 3.3), the crossover point is clearly visible. It is therefore true, that huge amount of nodes or very small parameter  $c$  is necessary to get the visible crossover point. On (Fig. 3.3) we can see that the  $k_{cross}$  point is not at the value of 200 predicted of the DM model. One can argue that this is due to the fact, that  $k_{cross}$  is calculated for the DM model and not for our model. Unfortunately, I was not able to find analytical prescription for the  $k_{cross}$  for our word web model (3.2).

For all networks, I have also measured the clustering distribution (2.7). I have found that in all cases power law tail is present in the distribution. For the generated networks the scaling exponent is, however, quite low ( $\approx 0.5$ ), indicating only a weak hierarchy for the well connected nodes (Fig. 3.2).

### 3.5 Conclusions

In conclusion, I have presented a model of growing network, that explains the difference between the exponent of the steeper part of the degree distribution predicted by the DM model [20] and the value measured by Cancho and Solé [15] in their positional word web. The model includes additional event, such as preferential edge rewiring (3.2). In the word web terminology this process means, that certain word loses one of its meanings, or contexts, and gains a different one.

Although this model of growing network was inspired by the language data, it has a general relevance to all networks growing by the included processes.

To verify the validity of the model for another real word webs, I developed positional word web for several English translations of The Bible. Using the network creating processes expressed by the model (3.2), I have generated several networks in which I first disallowed and then allowed multiple edges between nodes. For all networks degree distribution has been measured, showing no two scaling regimes (*Fig. 3.1*). I have shown numerically that there are two possible reasons for this. Either it is due to the small network size, or the parameter  $c$  is too big. The second regime appears in a network, if there are nodes with a higher degree than  $k_{cross}$  parameter (3.8) (*Fig. 3.3*). Because  $k_{cross}$  in (*Fig. 3.1*) is out of the  $k$  - range, we have to compare scaling exponents to  $\gamma_{DM}^1 = 1.5$ . For the BWW network the scaling exponent is close to 1.7, which is different from the predicted value. I do not know the reason of this discrepancy. It is possible, that BWW - s are too small to get a good and long enough linear part in the degree distribution, and thus more accurate  $\gamma$  measurement. From (*Fig. 3.1*) it is possible to see, that the  $\gamma$  exponents of artificial networks without multiple edges are closer to the theoretically predicted value 1.5. This is surprising, because theoretical models do not exclude multiple edges (2.26, 3.2). On the other hand, multiple edges were excluded during the creation of the BWW and prg networks. Measuring of clustering distribution (2.7) has shown that there is a weak hierarchical structure in all networks.

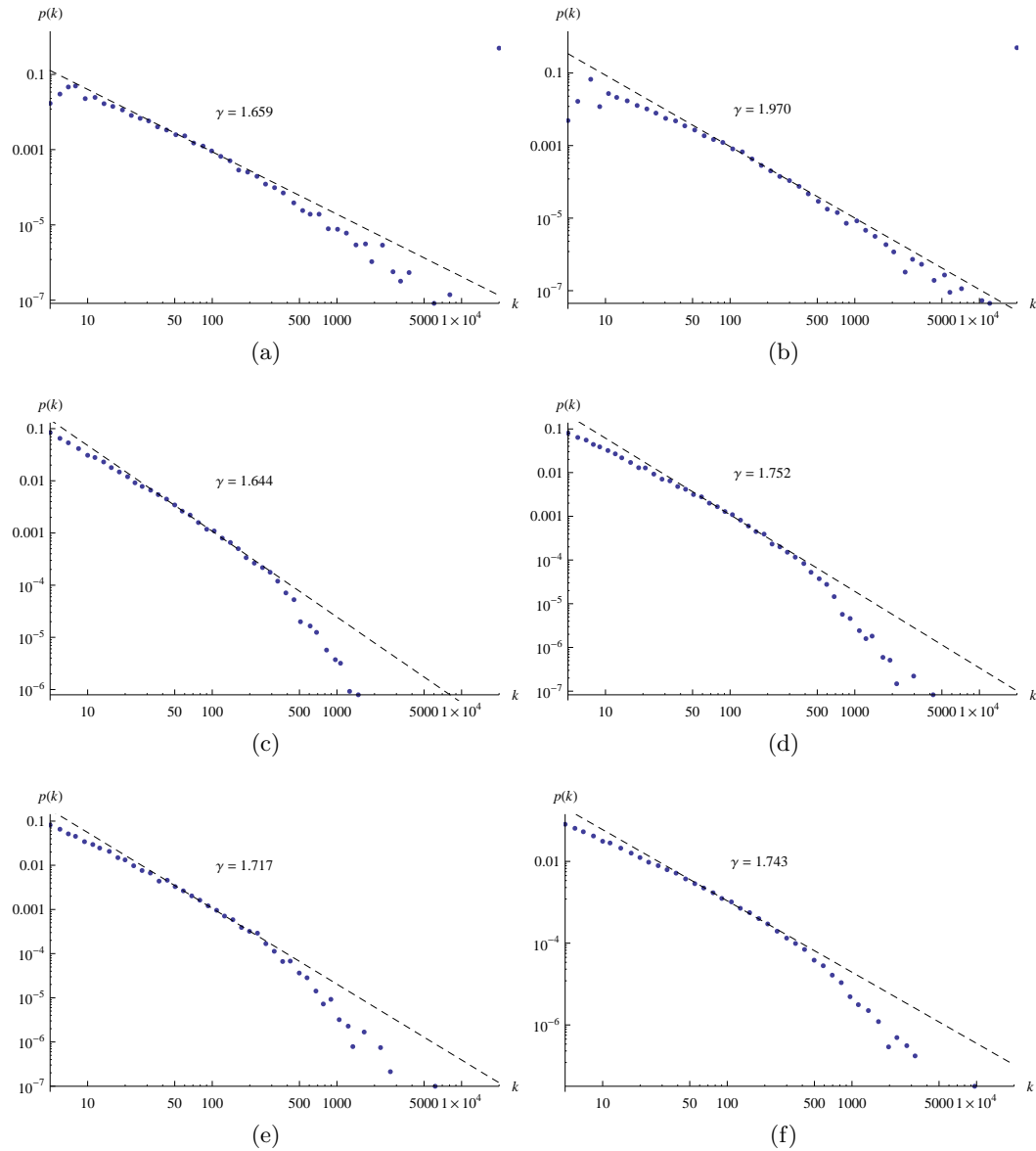


Figure 3.1: Log-log plot of degree distributions of the word webs, with their  $\gamma$  exponents. (a) kjv bible version network, (b) generated network (kjbGen), without multiple edges allowed (parameters were following:  $t = 11592$ ,  $m = 4$ ,  $c = 0.003$ ,  $m_r = 2$ ) (c) network generated with the same parameters, but multiple edges allowed (kjbGenME). (d) prg network. (e) generated network (prgGen), without multiple edges allowed (parameters were following:  $t = 21104$ ,  $m = 4$ ,  $c = 0.002$ ,  $m_r = 2$ ) (f) generated with the same parameters, but multiple edges allowed (prgGenME). Parameters of the generated networks were chosen to generate networks with the characteristics similar to the kjv and prg networks

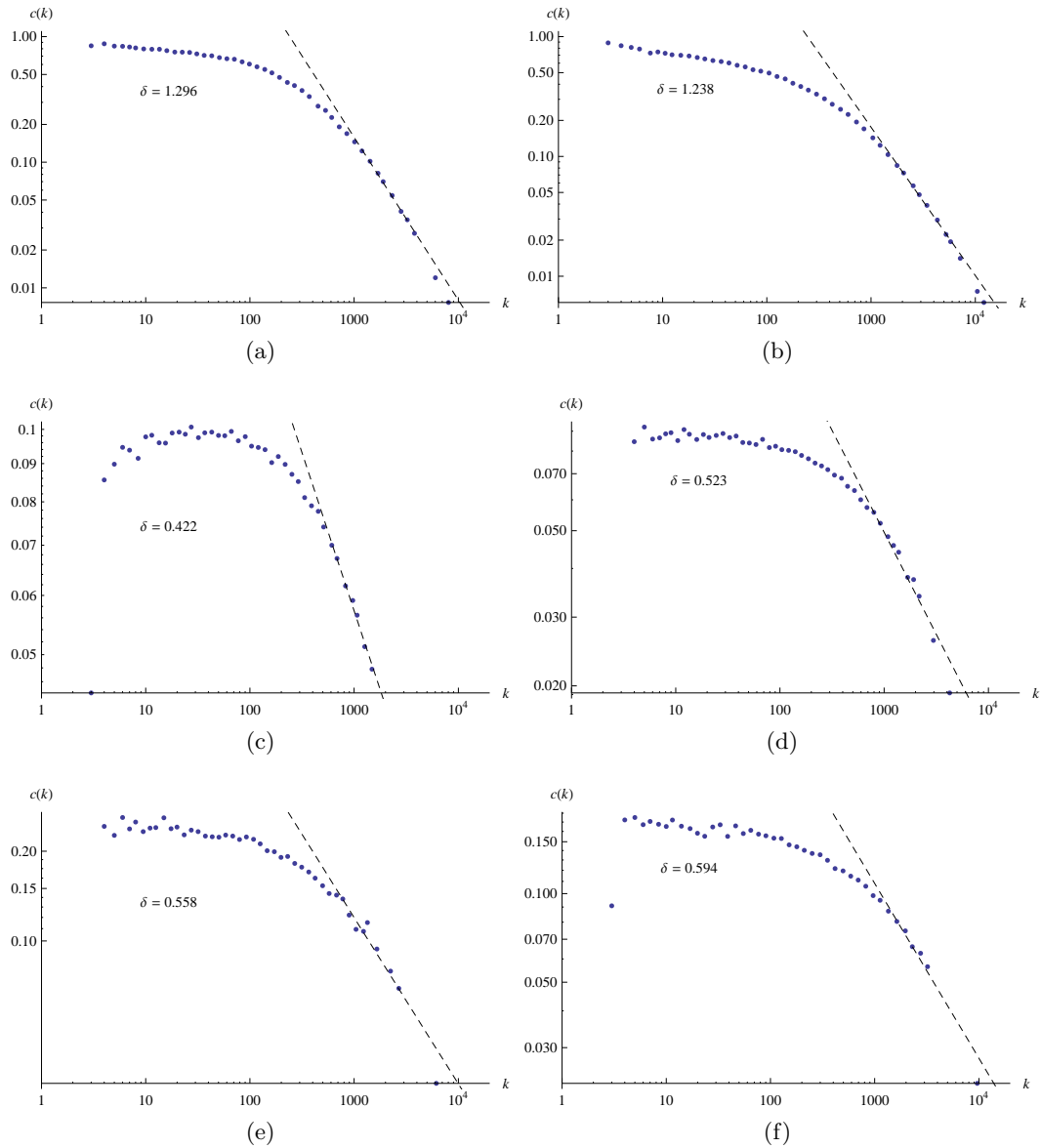


Figure 3.2:  $c(k)$  - clustering distribution of the word webs. (a) kjv bible version network, (b) generated network (kqvGen), without multiple edges allowed (parameters were following:  $t = 11592$ ,  $m = 4$ ,  $c = 0.003$ ,  $m_r = 2$ ) (c) network generated with the same parameters, but multiple edges allowed (kqvGenME). (d) prg network. (e) generated network (prgGen), without multiple edges allowed (parameters were following:  $t = 21104$ ,  $m = 4$ ,  $c = 0.0025$ ,  $m_r = 2$ ) (f) generated with the same parameters, but multiple edges allowed (prgGenME). Parameters of the generated networks were chosen to generate networks with the characteristics similar to the kjv and prg networks. All distributions have power law regime with for large  $k$ . Plots are in log-log scale.

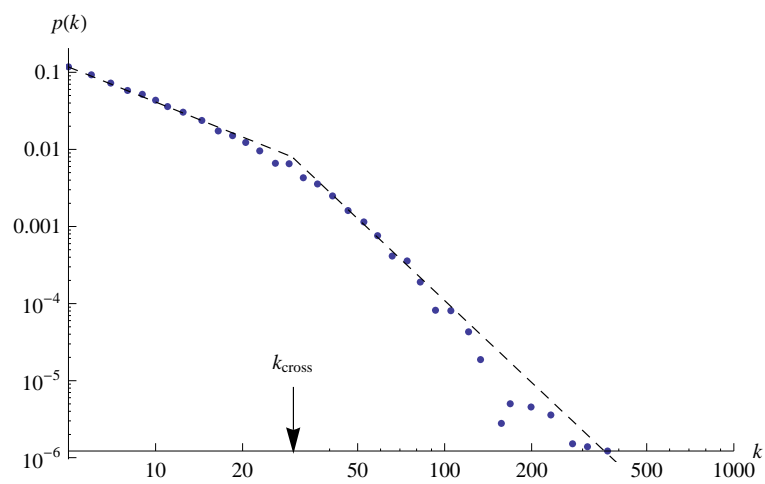


Figure 3.3: Log-log plot of the degree distributions of the generated network (gen20000) with no multiple edges. Parameters were:  $t = 20000$ ,  $m = 4$ ,  $c = 0.0003$ ,  $m_r = 2$ . With a low parameter  $c$ , the crossover point  $k_{\text{cross}}$  is present in the distribution.

## Chapter 4

---

# Clustering driven model

---

### 4.1 Introduction

Real networks often combine hierarchical structure with scale-free structure. BA model reveals how the latter emerges during the network evolution, but BA networks does not show any signs of hierarchy. Therefore natural question arises: Is there a special dynamical process creating hierarchy in the network? This question has been studied by Ravász and Barabási [51]. They speculated, that the hierarchy is established by iterative addition of a certain pattern, and proposed deterministic and randomized version of such addition. I described their model in chapter 2. They also found, that a power law analogical to (2.20) governs a scaling of clustering distribution.

$$c(k) \propto k^{-\delta}, \quad (4.1)$$

where  $\delta$  is a scaling exponent and  $c(k)$  an average clustering coefficient of nodes having the degree  $k$ . This is a significant difference from the Barabási - Albert model (2.3.3), in which average clustering coefficient  $c(k)$  does not depend on  $k$ , but is rather constant for all  $k$ -s.

In our studies [48] we examine, whether there exists another simple natural growth process resulting in the hierarchical scale free network structure. Similar models with local rules, but randomly driven, were studied by Vázquez [62]. In Section 4.2 I describe a simple clustering driven model. In collaboration with my co-workers I show analytically, that the pure clustering driven addition of nodes does not lead to the hierarchical scale free network structure. I agree with Vázquez [62], that local rules, regardless of the attachment kernel, are decisive. Nevertheless, our model is not the same as that of Vázquez. Detailed analytical and numerical studies of our clustering driven model as well as that with random

attachment kernel, are presented in section 4.3. Section 4.4 includes discussion and some concluding remarks.

## 4.2 The model

As described before (2.3.6), RB model reveals how hierarchy in the network is established. Nevertheless the process itself is somewhat artificial. It is difficult to find an equivalent of such strict pattern addition in the nature.

Models with local rules leading to the scale-free and hierarchical properties of networks were introduced by Vázquez [62]. This model has been described in Chapter 2. He describes mathematically how several surfers are exploring network structure by walking randomly on it. Description of Vázquez model, with a solution of this model using a continuous approach is in Section 2.3.7. My goal was to find a model inspired by more natural growth process (such as preferential attachment, for example), leading to the hierarchical network and to reveal the impact of local and global rules on the network structure. Here I describe our clustering driven model (CD model) [48]. The process is defined as follows:

1. We start from a small network, for example three completely interconnected nodes.
2. Then we add a new node at each time unit; it brings  $m > 1$  new edges into the system. Nodes are labeled by the time  $s$  in which they join the system.
3. One of the edges links itself to an old node  $s$  with the probability proportional to the clustering coefficient of the node  $s$ . Thus the linking probability of the new node  $s'$  to and old node  $s$  is

$$\Pi(s) = \frac{c(s)}{W(t)}, \quad (4.2)$$

with  $W(t) = \sum_{i=1}^t c(i)$ . The other  $m - 1$  edges are randomly distributed among the neighbours of the node  $s$ . To make the growing process independent of the initial module, we also use the attachment probability  $\Pi_{new}(s)$

$$\Pi_{new}(s) = \frac{1 + c(s)}{t + W(t)}. \quad (4.3)$$

Now, if the clustering coefficient of the node  $s$  is zero, there is still a probability  $\frac{1}{t}$  to choose it. Because each time unit one node comes to the system, at time  $t$  number of nodes in the network  $N(t) \approx t$ . For great  $t$  both  $\Pi$  (4.2) and  $\Pi_{new}$  (4.3) have the same behaviour, because  $W(t) = \bar{c}t$ , where  $\bar{c}$  is an average clustering coefficient of the network 2.5. I support this by

numerical simulations and I have shown that the behavior of CD model is the same for  $\pi$  and  $\pi_{new}$ .

This process might be an analogy of how the real groups of interest grow. Let us have, for example, a group of rambler. A new Rambler, wishing to join some group, often finds a central person leading a group and planning the trips, and, perhaps, contacts this person. This central person usually knows all key members and these key members form a dense cluster. Majority of them know each other, so the clustering coefficient of the central person is rather high, even close to one. When joining the group, a new member makes friends among other persons belonging to it. Of course, some of his (or hers) new friends are members of the other Rambler societies, or other groups of interests (photographers, tennis players etc.) and this way one gains contacts in the other clusters as well.

### 4.3 Results

Let me start the analysis of the CD model from its most simple variant. Initial network forms a small circle consisting of three nodes and three edges, all nodes thus having clustering coefficient one. Each time step one node and  $m = 2$  edges are added. One of the two edges links itself with the clustering preference to the older node  $s$ , the other chooses randomly between the neighbours of  $s$  (*Fig. 4.1*). In this simplified CD model (SCD model) the node  $s$  can thus gain a link by the two possibilities:

- By the clustering driven preference.
- In a case, that a node is a neighbour of another one, which has been chosen by the clustering driven preference.

Numerical studies show (*Fig. 4.2*), that such network has scale free hierarchical structure (2.7).

In this SCD model, node clustering coefficient is a simple function of the node degree

$$c(s) = \frac{2(k(s) - 1)}{k(s)k(s - 1)} = \frac{2}{k(s)}, \quad (4.4)$$

due to the fact, that each time a new triangle of nodes is created in the network. The number of edges among nearest neighbours of the node  $s$  at time  $t$  is  $k(s, t) - 1$ .

First let me show, that the clustering driven node addition itself is not responsible for the scale-free structure of the network. Here I present an analytical solution of the growing clustering driven network in which each time unit only one node and one edge is added. Node linking probability is proportional to  $k^{-1}$ . Average degree  $k(s, t)$  of the node  $s$  evolves with time  $t$  as

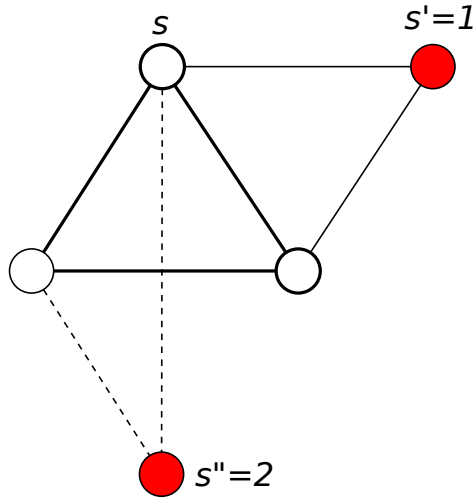


Figure 4.1: Node attachment in the SCD model. We start with a triangle (white nodes). Every node has a clustering coefficient equal to 1. In next time step, we attach node with index  $s' = 1$ , which brings two new edges ( $m = 2$  for the SCD model) marked with solid lines. Attaching an edge to an old node  $s$  is driven by clustering preference (4.2). Another edge is attached to the neighbourhood of the node  $s$ . The process continues further. In the CD model  $m - 1$  edges are added to the neighbourhood of the node  $s$ .

$$\frac{\partial k(s, t)}{\partial t} = \frac{k(s, t)^{-1}}{\int_1^t k(s, t)^{-1} ds}. \quad (4.5)$$

Let us suppose, that the solution of (4.5) has the form

$$k(s, t) = b[f(s) + g(s)]^\alpha \quad (4.6)$$

Then, with a help of the equation (4.5), we get

$$k(s, t) = [2^{\frac{1}{2}}[f(s) + g(t)]]^{\frac{1}{2}}. \quad (4.7)$$

where the expressions  $1 - \alpha = \alpha$  and  $b^2\alpha = 1$  are used. From the initial condition  $k(t, t) = 1$  and the equation (4.7) it is possible to derive, that  $f(s) = \frac{1}{2} - g(s)$ . Seeking  $g(t)$  in the form  $g(t) = \log_a(t)$  we finally have

$$k(s, t) = \left[ 2^{\frac{1}{2}} \left[ 1/2 - \log_a \left( \frac{t}{s} \right) \right] \right]^{\frac{1}{2}}. \quad (4.8)$$

and

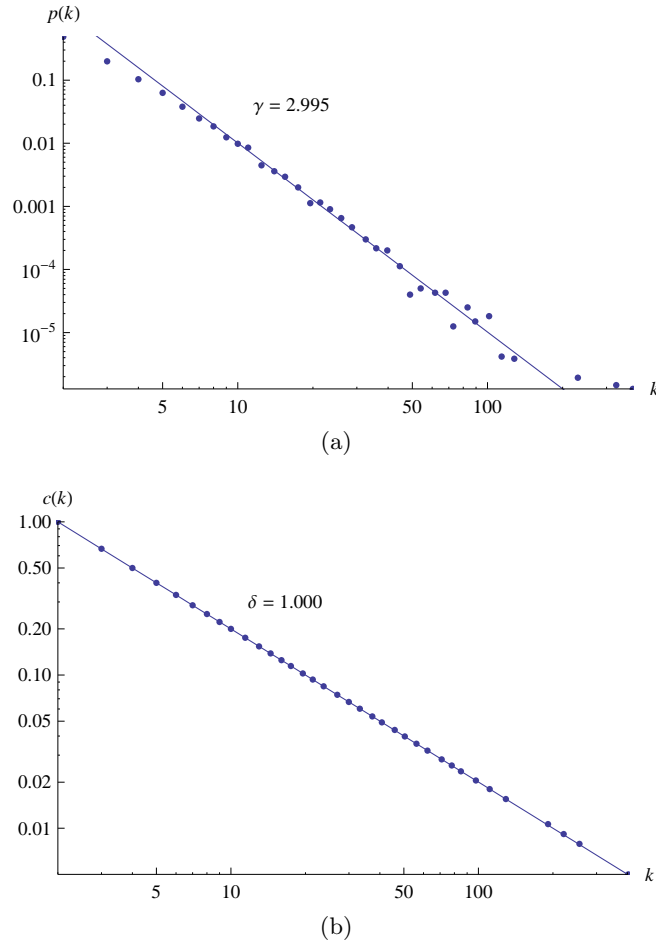


Figure 4.2: Log-log plots of the degree and clustering distributions for SCD model ( $m = 2$ ,  $N = 20000$ ).

$$g'(t) = \frac{1}{\int_1^t \frac{\ln^2(a) ds}{[\ln(a) + 2\ln(\frac{t}{s})]^{\frac{1}{2}}}} = \frac{1}{f(a) - (a\pi)^{\frac{1}{2}} t [Erf(d(a)^{\frac{1}{2}}) - Erf((d(a) + \ln(t))^{\frac{1}{2}})]}, \quad (4.9)$$

where  $f(a) = \frac{2^{\frac{1}{2}}}{\ln^2(a)}$  and  $d(a) = \frac{\ln(a)}{2}$ . For great  $t$  the error function  $Erf\left(\left(\frac{\ln(a)}{2} + \ln(t)\right)^{\frac{1}{2}}\right) = 1$  and from the equation (4.5) we find that  $a = 2.964$ . It is well known that such solutions as (4.8) do not lead to the power law degree distribution, but the distribution decreases exponentially [3]. We can therefore state, that the clustering driven node linking preference itself is not responsible for the scale-free network structure.

SCD model can be compared to the model of Vázquez (2.3.7) with only one surfer and the probability one, that a visited vertex increases its degree by one. The SCD model differs from that of Vázquez, by the way of the edge addition. In the most simplified version of the V model, each time unit one edge or one edge and one node is added. We can compare the SCD model with a simplified V model, where the parameter  $q_e$  (the probability of following an edge from selected node) is set to  $\frac{1}{2}$ , because we add two edges in one time unit. SCD model also introduces the clustering driven preference (4.4) into the rate equation (2.38). Having in mind the above mentioned facts, the probability  $A_k$  (that the degree of a vertex of degree  $k$  increases by 1 when a surfer walks on the graph) in our SCD model is:

$$A_k = \frac{1}{N} \left[ (1 - q_e) \frac{2}{k\bar{c}} + q_e v_a k \right], \quad (4.10)$$

where  $\bar{c}$  is an average clustering coefficient (2.5) and  $q_e = \frac{1}{2}$ .

Analogically, as in 2.3.7, using the fact that  $v_s = 1$ , and introducing (4.10) in (2.38) we get the equation from which we are able to derive the degree distribution

$$\frac{\partial Np(k)}{\partial t} = - [A_k Np(k) - A_{k-1} Np(k-1)] + v_a \delta_{k,0}. \quad (4.11)$$

For large  $k$  we can use a continuous approach and with the help of (2.34) and (4.10) rewrite the equation (4.11):

$$\frac{\partial Np(k)}{\partial t} = - \frac{\partial A_k Np(k)}{\partial k}, \quad (4.12)$$

$$v_a p(k) = - \frac{\partial [q_v(1 - q_e)/(2k\bar{c})p(k) + q_e v_a k p(k)]}{\partial k} \quad (4.13)$$

$$\frac{\partial p(k)}{\partial k} = p(k) \frac{v_a(1 + q_e) + \frac{2(1-q_e)}{k^2\bar{c}}}{(q_e - 1)\frac{2}{k\bar{c}} - q_e v_a k}. \quad (4.14)$$

For  $q_e = 0$ , these equations describe the same model as in (4.5) In this model only one node and one edge with a preference proportional to  $k^{-1}$  are added at each time unit. The solution of (4.14) with  $q_e = 0$  shows directly that the clustering driven term of  $A_k$  is not responsible for the scale-free structure of the network.

For  $q_e \neq 0$  the solution of this equation (4.14) is

$$p(k) \propto k^{-\gamma}, \quad \gamma = 1 + \frac{1}{q_e} \quad (4.15)$$

which also agrees with the solution of Vázquez [62].

As stated before, in the SCD model, clustering coefficient is given by the equation (4.4). From (4.4) and (4.1) it is obvious, that the scaling exponent  $\delta = 1$ . This was also verified by numerical simulations (Fig. 4.2).

The generalized clustering driven model (CD model) with  $m > 2$  links added at each time step has been studied numerically. I have developed a network with  $N = 20000$  nodes and  $m = 3$ . The significant difference of our model and that of Vázquez [62] is, that in the Vázquez model, the exponent of the degree distribution  $\gamma$  depends on the parameter  $q_e$  (4.15). In our model, as  $m$  grows, scaling exponent  $\gamma$  quickly adjusts itself to the value  $\gamma = 3$ . This holds even for the randomly driven model where the clustering preference is replaced by a random choice (Fig. 4.6b). The reason is simple. Number of edges in the Vázquez model changes with time as

$$\frac{\partial E}{\partial t} = \bar{v}N. \quad (4.16)$$

where  $\bar{v} = q_e \frac{\bar{k}}{N}$ . In CD model each time unit a fix rate of edges ( $m > 2$ ) is added. That means that the equation (4.16) is rewritten as

$$\frac{\partial E}{\partial t} = m = q_e \bar{k}. \quad (4.17)$$

It is easy to calculate the average degree  $\bar{k}$  for our model.

$$\bar{k} = \frac{\sum_i^N k_i}{N} = \frac{2mt}{t} = 2m. \quad (4.18)$$

Incorporating this equation into (4.17) we get, that  $q_e$  for all  $m$  is

$$q_e = \frac{m}{\bar{k}} = \frac{m}{2m} = \frac{1}{2}, \quad (4.19)$$

That means that the degree distribution scaling exponent  $\gamma = 3$  (4.15), as it is also confirmed by the numerical simulations (Fig. 4.4a).

For the CD network, I have calculated numerically an average clustering coefficient  $\bar{c}$  and found, it to be rather high,  $\bar{c} = 0.6$ . I checked its independence of the network size and examined the small world properties of the network. Separation of nodes (2.1) changes with system size as  $\ell \propto \log(N)$  (Fig. 4.3), confirming the small world network structure.

As it was written before, our clustering driven process leads to the scale free network with hierarchy. It is also true for the same process with random attachment kernel. These facts are reflected in the power law scaling of  $p(k)$  and  $c(k)$  (Fig. 4.4, 4.7, a, b), (4.1, 4.15), where  $\gamma$  exponent is independent from the number of new edges  $m$  (Fig. 4.6b, 4.7c). On the other hand exponent  $\delta$  seems to decrease with  $m$  as  $m^{-\alpha}$ , where  $\alpha = 0.1$  (Fig. 4.6a).

To check how the properties of CD model depend on the initial conditions, I have evaluated our model with  $\pi_{new}$  for a set of initial modules (star, circle, triangle). I have found that  $\gamma$  and  $\delta$  exponents are independent of the initial conditions.

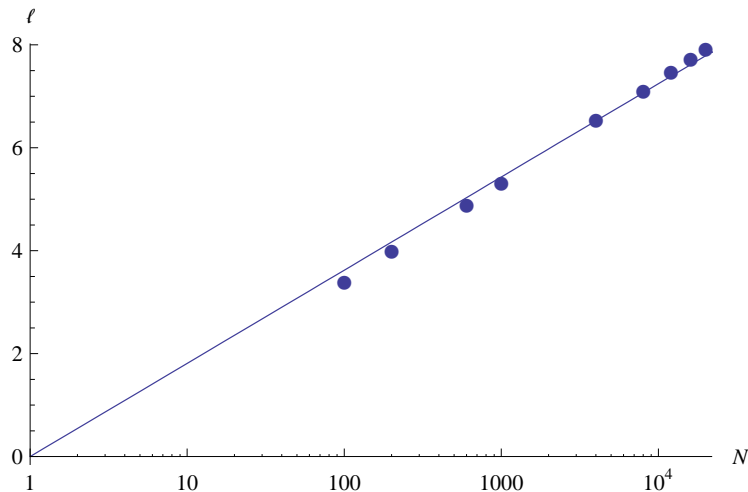


Figure 4.3: The dependence of the  $\ell$  on the system size for CD model.  $N$  is the size of the network. The line represents  $\frac{1}{2}\log(N)$  in the log-linear plot.

How does our network look visually? To show this, I have visualized both CD models with  $\pi$  and  $\pi_{new}$  for the same  $m$  and in the same stages of development (*Fig. 4.5*). CD models with  $\pi$  and  $\pi_{new}$  does not seem to show any visual differences. The visualization has been made with a help of Network Workbench tool [58].

To conclude this section, I agree with Vázquez, that independently of the node attachment kernel, local rules are decisive for the scale free property and hierarchy in the final network topology. It is due to the fact, that the local rule introduces effective preferential attachment [62]. When new node comes to the system, it adds new edges to the neighbours of some old node. Thus the nodes with more neighbours (higher node degree) have better chance to gain a new edge. This was an effective preferential attachment introduced to the CD model.

## 4.4 Conclusions

I and my co-workers propose a clustering driven model of growing network (CD model). We have found, that simplified version of this model can be compared to the Vázquez network with the parameter  $q_e = \frac{1}{2}$ , one surfer and the probability of new link addition equal one (V model) [62].

Difference in CD and V model lies in the node and edge adding rule. In our CD model, each time unit one node and a fixed ratio of edges come to the system. This is not true for the V model. In the CD model we use the clustering preference for the new node linking, but as I have shown, this is not substantial. Degree distribution of the clustering driven model and the model with random

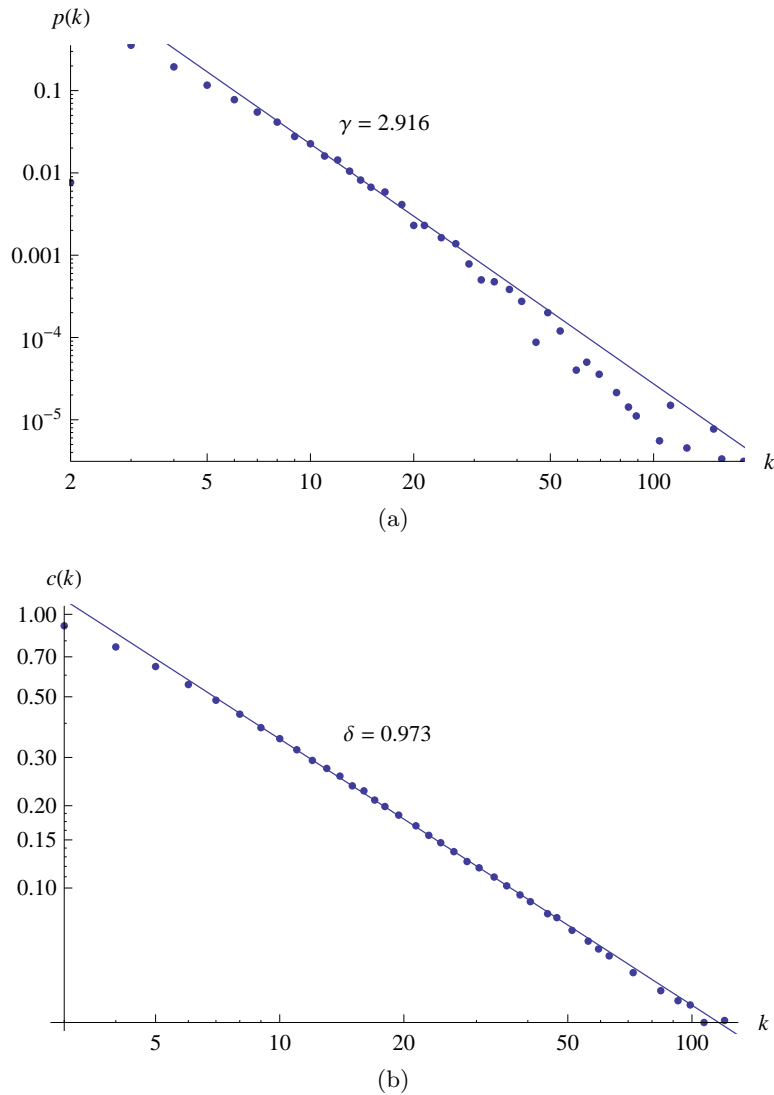


Figure 4.4: Degree (a) and clustering (b) coefficient distribution for CD network:  $N = 20000$  nodes,  $m = 3$  and attachment probability  $\pi_{new}$ . Both plots are log-log.

preference scales as  $p(k) \propto k^{-\gamma}$ , where  $\gamma = 3$ . Nevertheless these models differ from that of Vázquez [62]. Together with my co-workers, I have shown analytically that exponent  $\gamma = 3$  is independent on the other network parameters, contrary to the V model, where  $\gamma = 1 + \frac{1}{q_e}$ ,  $q_e$  being the probability of surfer to follow a link incident to the chosen node.

In the numerical studies of the CD model, I have shown that the growing process creates a network with hierarchy, as well as the scale free property. Such networks are ubiquitous in the nature, even more than simple scale free nets lacking hierarchy in node ordering.

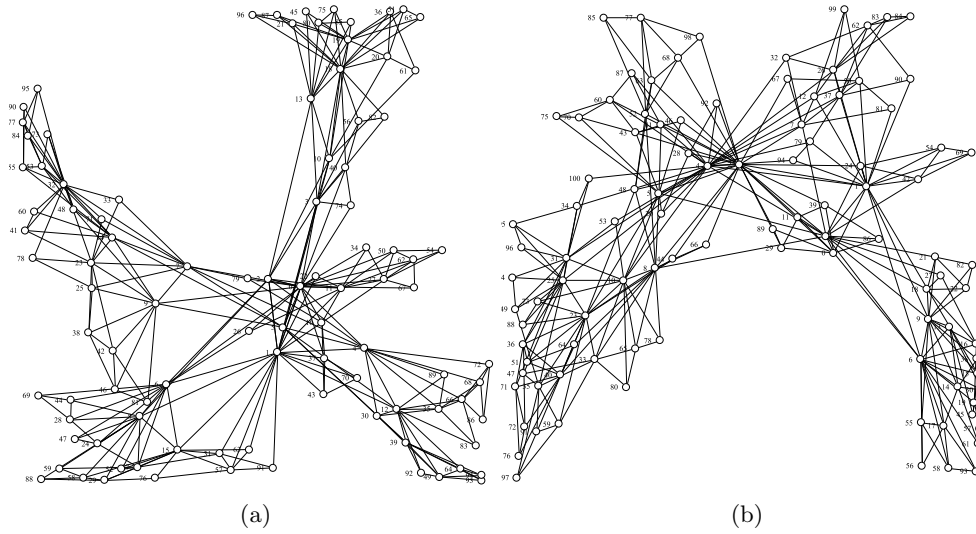


Figure 4.5: Visualization of CD networks. (a) CD model with attachment probability  $\pi$ . (b) CD model with attachment probability  $\pi_{new}$ . Number of nodes in both networks is 100 nodes and the parameter  $m = 3$ .

In agreement with Barabási and Ravász I have shown, that addition of a certain pattern is necessary to establish a hierarchy in the network. However, this pattern does not consist of a fixed module. It is rather created naturally by connecting  $m - 1$  neighbours of aSSS certain node  $s$  to a new coming node  $s'$ . I also agree with Barabási and Ravasz that the  $\delta$  exponent (4.1) is  $m$  dependent and thus non universal. I have shown numerically, that both  $\gamma$  and  $\delta$  exponents are independent of the initial conditions.

To summarize, we have found a process which leads to the hierarchical scale free network. In this process local rules pre-dominate the global rules of choosing a new node.

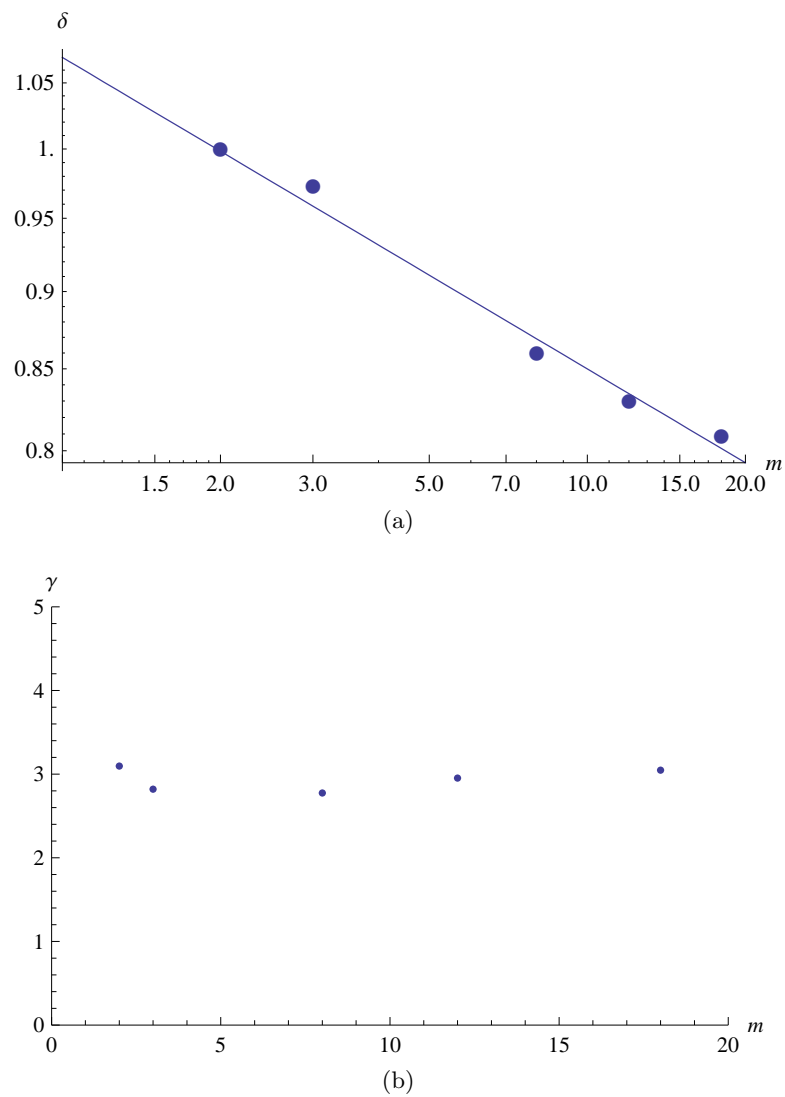


Figure 4.6: (a)  $\delta$  dependence on the number of new edges  $m$ .  $\delta$  decreases with  $m$  as  $m^{-\alpha}$ , where  $\alpha = 0.1$ . (b)  $\gamma$  dependence on the number of new edges  $m$ . Calculated for CD network with 20000 nodes, attachment probability is  $\pi_{new}$ .

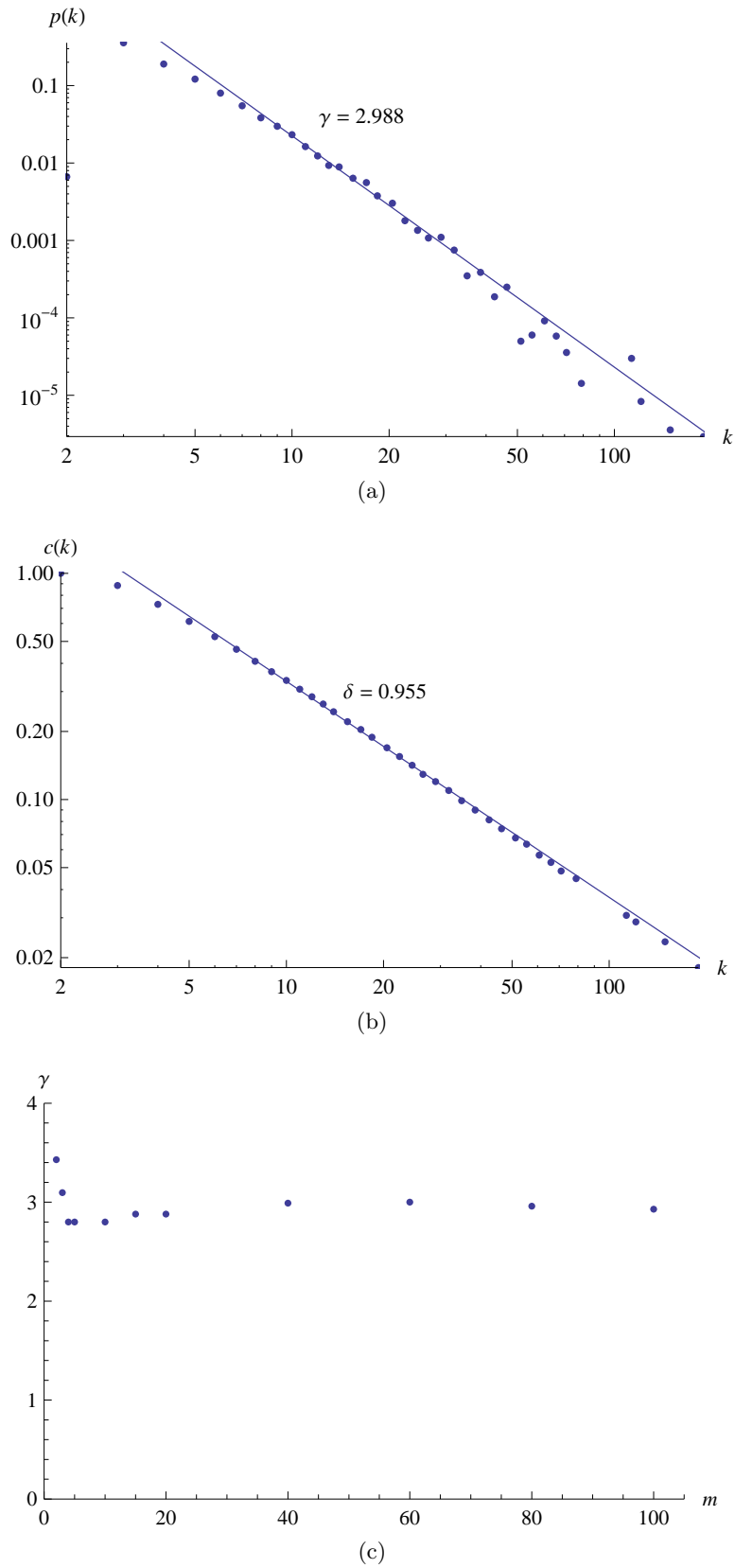


Figure 4.7: Random model with the local rule. At each time a node is attached and connected with an edge to one randomly chosen existing node  $s$ . Then it is connected with  $m - 1$  nodes in the neighbourhood of the node  $s$ . Network has  $N = 20000$  nodes, parameter  $m = 3$ . (a) degree distribution, (b) the dependence of the clustering coefficient on the node degree (c) the dependence of the degree distribution exponent  $\gamma$  from the parameter  $m$ . All plots are in the logarithmic scale.

## Chapter 5

---

# Functional brain networks

---

### 5.1 Introduction

Complex network theory is not only theoretically interesting, but has also practical applications. To study a model is useful, because with a help of the model one can explain properties of various real networks. For example a small-world model was successful in an effort to improve the performance of the routing in the peer-to-peer Freenet network [67]. High ability of using local information to find a target in semiinformative search reported by Milgram [44] was used to find a decentralized search algorithms, working for example on the US airline network [59]. Models of complex networks were successfully used to model network of Internet routers [27, 66], word wide web [4], language networks [15, 40, 20], protein interactions [45], large social networks in investigation and optimization problems relating to the spread of information or diseases in these networks [63, 57], composing music using structures found in compositions of famous artists [60] and many others [52, 6, 3]

One of many areas, where complex networks can help to understand the structure and processes behind, are functional brain networks [16]. Brain functional networks are extracted from functional magnetic resonance imaging (fMRI). fMRI is a technique of in vivo brain activity imaging [33]. It measures the blood oxygenation level dependent (BOLD) signal, related to neural activity in the brain. Signal from the whole brain is recorded sequentially in slices of thousands of voxels (*Fig. 5.2*). fMRI data are used to visualize the brain activity, to study the structure and active voxels under various conditions, localize brain areas responsible for different functions of the brain [56]. In addition, it is possible to analyze the data to seek the underlying functional brain networks, i.e. networks of functional units that temporarily self-organize themselves to engage in a given task or to engage in spontaneous background activity during the rest condition [16]. Geisel

et. all [19] and later Chialvo et. all [16] used graph theory to study the structure of functional brain network. These networks should depict the functional dependency between different voxels. To create a network from the measured data, one considers voxels to be nodes of the network, link between two voxels is created if their activities are well correlated through time. Some studies have shown that functional brain networks have characteristics of small world networks and that they have power law degree distributions which indicates the scale-free structure [16, 2, 61].

In [41] possible differences between functional networks for brain in different states of activity or performing different tasks were studied. It was reported that the scale-free structure, reflected by the linear part of the log-log plot of degree distributions is more pronounced for the brain performing a given task than for the brain in a resting state. This means that during the simple motor task of finger tapping, the structure of the network was more complex [41]. These results were obtain on networks created upon random sampled subset of voxel pairs. Here I show extended analysis of the same data using all vector pairs as possible candidates for connection.

In this chapter I will also present a case study of functional brain networks of old people with dementia. It is known that the structure of the brain is affected by dementia [8, 65]. The question is whether the topology of functional brain networks reflect this fact. Study on differences in functional brain networks of young, nondemented and demented adults was also performed by Buckner [14]. However, topological characteristics as small-worldness or degree distribution or hierarchicity were not examined. My analysis on their data fills the gap. Here I would like to state, I got the data with a help of Dr. Liz Franz and Dr. Lubica Benušková from the University of Otago, Dunedin, New Zealand.

## 5.2 Network construction and analysis

Output of fMRI brain imagining consists of voxel activity record. Voxel is a part of a brain, having approximately  $3mm^3$ . The activity is recorded in slices. Slices are recorded sequentially and one scan takes approximately 2 seconds. Voxels are real 3D points in the brain, containing several neurons.

Position in space or anatomical connections among neurons suggest direct ways to create networks. However, as I mentioned above, intention of functional brain networks is to reflect the mutual dependency of voxel activities. During experiment, scans were repeated periodically. Thus for each voxel we have a vector of activities in different time points. To create a functional network we take each voxels as a node in a graph. The functional dependency of two voxels is expressed by creating an edge between them. Let us have a function  $f(x, y)$  that defines relation between voxels  $x$  and  $y$  represented by vectors of their intensities in

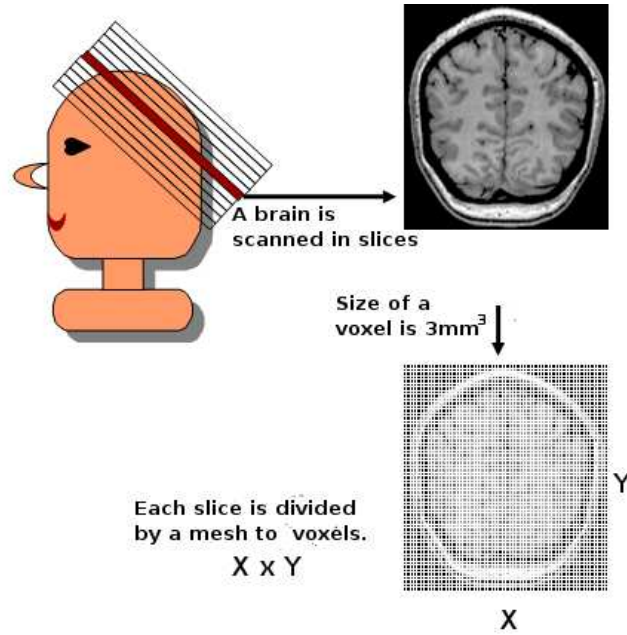


Figure 5.1: fMRI experiment. A brain is scanned in slices, that are few millimeters thick. Each slice is divided by a mesh to voxels. Size of one voxel is  $3mm^3$ . Result of scanning is set of voxel activities for each scanned slice [39].

different time points. We say that there is a 'functional' connection between voxel  $x$  and voxel  $y$  if  $f(x, y) > r$ , where  $r$  is a threshold parameter of the functional brain network. Graph of a functional brain network  $FBN(V, f, r)$  underlined by a set of voxels  $V$ , is defined as follows:

**Definition 2.**  $FBN(V, f, r) = \{V, E\} = \{(x, y) | x \in V \wedge y \in V \wedge f(x, y) > r\}$ ,

where  $V$  is a set of nodes and  $E$  set of edges of the graph. Thus the algorithm to create a graph is straightforward:

- For each pair of voxels  $x$  and  $y$  calculate the function  $f(x, y)$ . If the calculated value is larger than parameter  $r$ , create an edge between voxels  $x$  and  $y$ .

Usually a Pearson correlation coefficient is used as a function  $f$  [16, 41]. Pearson correlation of two random variables  $X$  and  $Y$  is defined as

$$\rho(X, Y) = \frac{cov(X, Y)}{\delta x \delta y}, \quad (5.1)$$

where  $cov$  is covariance and  $\delta x$  and  $\delta y$  are standard deviations. If we have two variable samples (voxels intensities over time in our case) with  $n$  measurements

of  $X$  and  $Y$  written as  $x_i$  and  $y_i$  where  $i = 1, 2, \dots, n$  then the sample correlation coefficient, can be used to estimate the Pearson correlation between  $X$  and  $Y$ :

$$\rho(X, Y) = \frac{n \sum x_i y_i - \sum x_i \sum y_i}{\sqrt{n \sum x_i^2 - (\sum x_i)^2} \sqrt{n \sum y_i^2 - (\sum y_i)^2}}. \quad (5.2)$$

In my analysis I consider also anticorrelation (correlation is lower than some negative threshold) as a candidate for an edge. Thus, we can write the function  $f$  as

$$f = |\rho(X, Y)| = \left| \frac{n \sum x_i y_i - \sum x_i \sum y_i}{\sqrt{n \sum x_i^2 - (\sum x_i)^2} \sqrt{n \sum y_i^2 - (\sum y_i)^2}} \right|. \quad (5.3)$$

Inspired by previous work on the analysis of functional brain networks [53] I used Granger causality as other measure for the selection of the function  $f$ . Granger causality is a statistical concept of causality that is based on prediction. According to Granger causality, if a signal  $X$  "G-causes" a signal  $Y$ , then past values of  $X$  should contain information that together with past values of  $Y$  help to predict values of  $Y$ . Its mathematical formulation is based on linear regression modelling of stochastic processes [30].

G-causality is normally tested in the context of linear regression models. For illustration, consider a bivariate linear autoregressive model of two variables. Model  $M_{xy}$ :

$$X(t) = \sum_{j=1}^p A_{1,j} X(t-j) + \sum_{j=1}^p A_{2,j} Y(t-j) + E_{XY}(t) \quad (5.4)$$

Model  $M_x$ :

$$X(t) = \sum_{j=1}^p B_{1,j} X(t-j) + E_X(t) \quad (5.5)$$

where  $p$  is the order of the model. Matrixes of coefficients ( $A, B$ ) describe the contributions of each lagged observation to the predicted values of  $X(t)$ .  $E_{XY}$  and  $E_X$  are residuals (prediction errors) for each model. If the variance of  $E_X$  (model  $M_X$ ) is reduced by the inclusion of the  $Y$  terms (model  $M_{XY}$ ), then it is said that  $Y$  (or  $X$ ) G-causes  $X$ .

The Granger causality between  $X$  and  $Y$  can be tested by performing an F-test of the null hypothesis that  $A_2 = 0$ . As the Granger causality is directed value, we considered one direction of the Granger causality ( $X$  G-causes  $Y$  or  $Y$  G-causes  $X$ ) as sufficient to create an edge. The  $n$  for the function  $f$  we have used

$$f = \max(F_{XY}, F_{YX}). \quad (5.6)$$

where  $F_{XY}$  ( $F_{YX}$ ) denotes value of the F-test that  $Y$  ( $X$ ) granger causes  $X$  ( $Y$ ).

In my measurements I have tried several values for the threshold parameter  $r$ . I have started with small values of the parameter  $r$  which led to the networks with almost all possible edges present. Networks became disconnected on a certain value of the parameter  $r$ . Then I chose this value as the final value for the threshold parameter  $r$ .

From the visualization of one slice of measured fMRI data, mapped to the brain (*Fig. 5.2*) one can see than only a small part of voxels is active. However in the measured data, almost every voxel has some very low non-zero intensity. These are often voxels outside the brain region. Draining veins oxygenation causes high voxel intensities[49]. To avoid these noisy effects one can set up thresholds to remove voxels with too low and too high intensities from data.

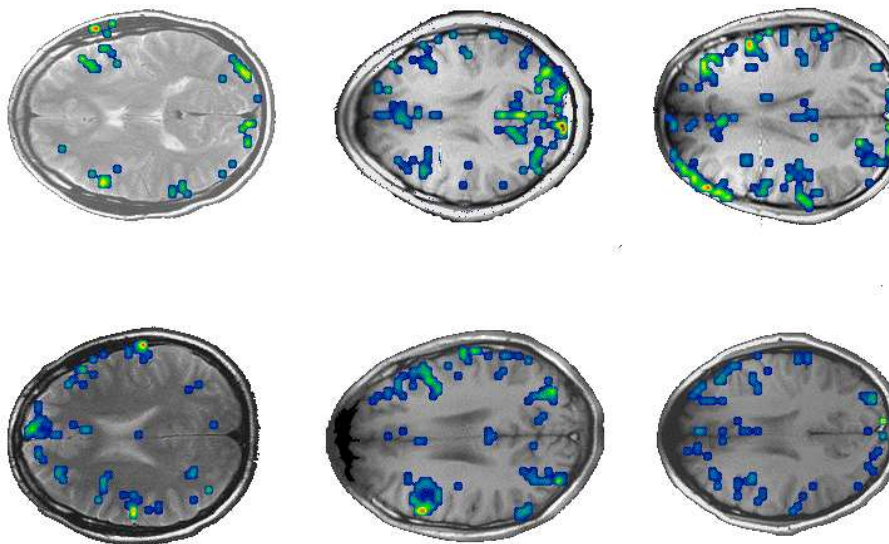


Figure 5.2: Regional voxel activation associated with a Stroop task (naming of colors) [55]. Six participants were scanned. Each plot represents one person. [29]

The question is how to determine these thresholds. On (*Fig. 5.3*) is a plot of the distribution of the average voxel intensities. Data came from the experiment on the University of Otago, where subjects were measured during active (test) and resting phase. Most of the voxels have intensity lower than 100 units (and most of these are zeroes), however, there is a peak around the intensity of 350 units. My idea was to incorporate only voxels with the intensity around this peak, as these

should be the voxels most involved in the brain activity. I discussed this idea with Dr. Liz Franz from the University of Otago who was making these experiments. In distributions depicted on (*Fig. 5.3*) voxels with the intensity between 200 and 600 units represent 15% of all voxels.

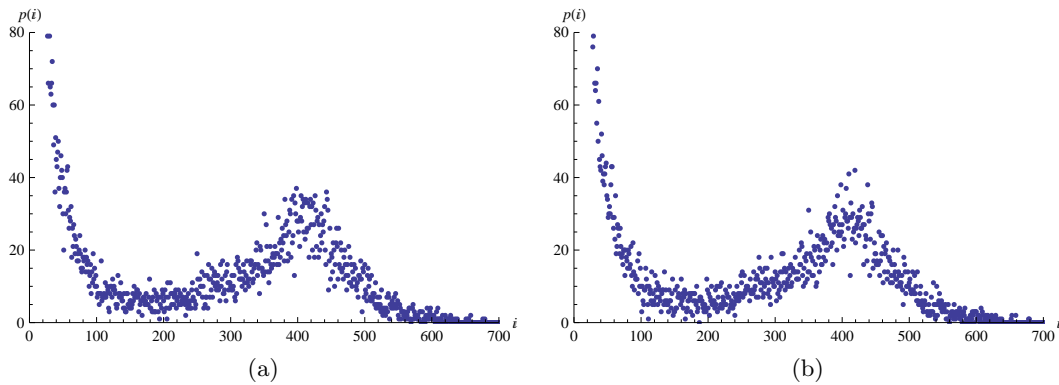


Figure 5.3: Distribution of average voxel intensities during rest (a) and test (b) phase. Distributions are joined through 4 subjects. Data are from an experimental series of a sample database associated with fMRIotago, Dunedin, New Zealand (see 5.3).

### 5.3 Active and resting functional brain networks

Markošová et. al [41] have extracted functional brain networks from fMRI data based on temporal correlations of voxel activities during the rest and test periods. In their experiment subjects performed simple finger tapping task during the test phase. The test phase was followed by the rest period in which brain relaxes doing nothing. fMRI scans were taken several times during each of these periods. Thus the functional brain networks for these two periods could be created. They studied the topology of these networks in terms of small-world and scale-free properties. The small-world property of generated functional brain networks was quite clearly evident whereas the scale-free character was less obvious. There were some differences between the rest and test functional brain networks. The scale-free properties were more pronounced in the test phase of measurement. This effect is clearly visible for the measurement of all four persons. However, they used only 80 million randomly chosen voxel pairs as edge candidates. Here I am presenting a new analysis of their data using all possible voxel pairs. In addition I also analyzed the data with the help of the Granger causality. To filter out only active voxels I took into account only voxels around the peak emerged in the distribution of voxel intensities, as described in section 5.2 (*Fig. 5.3*).

### 5.3.1 Material and methods

FMRI data came from an experimental series of a sample database from the University of Otago, Dunedin, New Zealand. Four subjects were scanned. Data were acquired during initial rest cyclus (16 seconds) when the measured person was asked to do nothing. This initial period was followed by 6 cycles of test (20 seconds) and rest (20 seconds). The first, 16 seconds long rest period was not considered for network creation. The task was a bimanual finger tapping, in which subjects tap once per second using thumb-index finger opposition movements. Subjects were tapping with both hands according to a 1 Hz tone signal. The tone remains on for test and rest period with a change in pitch. Each rest/test epoch contains 32,728 voxels [(Z = 1 to 8 slices) (X = 64) (Y = 64)], with 10 acquisition cycles with 2 s TR (i.e., 20 s epoch) [41].

In order to emphasize the signal features I have averaged the data in all rest and test periods for each subject. Plotting joined voxel intensity distribution for rest and rest periods has shown that in both distributions there is a peak present at size of 350 units (*Fig. 5.3*). Considering voxels around these peaks (intensities in range from 200 to 600) we have chosen 15% of all voxels to create functional brain networks.

I have created two networks for each subject. First using the Pearson correlation as function  $f$  (2), with the threshold  $r = 0.9$  and the other using the Granger causality with the threshold  $r = 50$ . For each network I have calculated small world characteristics such as node separation (2.1), and the average clustering coefficient(2.5). I have also studied degree distribution (2.6) to determine whether the networks have scale-free character. In addition to the original analysis [41] the clustering distribution (2.7) was measured. This measure, as described in Chapter 2, indicates hierarchical network structure.

### 5.3.2 Results

Results of my analysis are shown in the Table 5.1(for Pearson correlation (5.3)) and in the Table 5.2 (for Granger causality (5.6)). To verify the small-world property I have calculated the average clustering coefficient and the node separation of all networks.  $\bar{c}_{random}$  (2.14) for this graphs is  $10^{-3} - 10^{-4}$  and  $\ell_{random} \approx 4$  (2.13) for the graphs with the same size and average degree. Using these values I have calculated the small-world index (2.8) for networks created using Pearson correlation, which is rather high ( $si \sim 100$  to 300). Surprisingly the average clustering coefficient for the networks based on the Granger causality is very low ( $\sim 10^{-3}$ ) and thus the small-world index is only  $\sim 1$ . Low node separation with a low clustering coefficient resembles more random than small-world networks. I have

calculated the degree distribution for all subjects and both test and rest conditions. I have found the power law scaling with the scaling exponent  $1.1 < \gamma < 3.3$  ( $1.9 < \gamma < 5.7$ ) for Pearson correlation (Granger causality). This confirms the scale-free property. As in the original study [41], I did not discover any significant difference between the values of  $\gamma$  for the test and rest condition in individual subjects. Nor the differences were noticed between the rest and test conditions for certain subjects. This indicates similar scale-free structure of the network in both conditions.

network	$N$	$\bar{c}$	$\ell$	$\bar{k}$	$\gamma$
otago1-pearson-0.9-rest	4901	0.375	5.49	35	1.370
otago1-pearson-0.9-test	4869	0.289	7.41	12	1.193
otago2-pearson-0.9-rest	4302	0.262	6.77	11	1.803
otago2-pearson-0.9-test	4304	0.283	5.99	21	1.417
otago2-pearson-0.9-rest	3446	0.246	8.77	5	3.257
otago3-pearson-0.9-test	3491	0.245	9.75	5	1.848
otago4-pearson-0.9-rest	3819	0.263	7.14	8	2.031
otago4-pearson-0.9-test	3834	0.267	7.87	9	2.106

Table 5.1: Properties of functional brain networks based on Pearson correlation (5.3) with the threshold  $r = 0.9$ . Here  $N$  is the number of selected voxels,  $\bar{c}$  is the average clustering coefficient,  $\ell$  the node separation,  $\bar{k}$  the average node degree,  $\gamma$  the scaling exponent of the degree distribution. For each subject a rest and test networks were created.

network	$N$	$\bar{c}$	$\ell$	$\bar{k}$	$\gamma$
otago1-granger-50-rest	5517	0.002	4.71	18	1.961
otago1-granger-50-test	5534	0.001	5.07	8	2.950
otago2-granger-50-rest	4978	0.001	5.38	6	3.185
otago2-granger-50-test	5000	0.002	5.00	8	3.219
otago3-granger-50-rest	4279	0.0009	6.15	5	5.667
otago3-granger-50-test	4291	0.001	5.98	5	5.324
otago4-granger-50-rest	4389	0.001	5.55	6	4.326
otago4-granger-50-test	4452	0.001	5.66	5	5.294

Table 5.2: Properties of functional brain networks based on Granger causality (5.6) with the threshold  $r = 50$ . Here  $N$  is the number of selected voxels,  $\bar{c}$  is the average clustering coefficient,  $\ell$  the node separation,  $\bar{k}$  the average node degree,  $\gamma$  the scaling exponent of the degree distribution. For each subject a rest and test networks were created.

I can confirm the results from [41]. There is a difference between the shape of

the degree distribution for averaged rest and test periods for the networks created using the Pearson correlation. Scale-free structure, reflected by the linear part of the log-log plot is more pronounced for the test period (*Fig. 5.4*). We can see that the linear part in the degree distribution of the network constructed from data obtained during test period covers longer range (degree  $k$  from 10 to 80) than the network from the data obtained during the rest period (degree  $k$  from 10 to 180). However, more detailed studies are necessary to decide whether the short linear part is significant for the rest phase. Also, in this stage of my research, I am not able to decide whether the lack of differences between the topology of networks in the rest and the test phase is caused by the fact that the analyzed functional brain networks did not have enough nodes. The other possibility is that there is no real difference between the functional networks in different phases. I did not observe any difference in the topology for networks based on the Granger causality (*Fig. 5.5*). Even the more pronounced linear part of the test period degree distribution was not present in these networks.

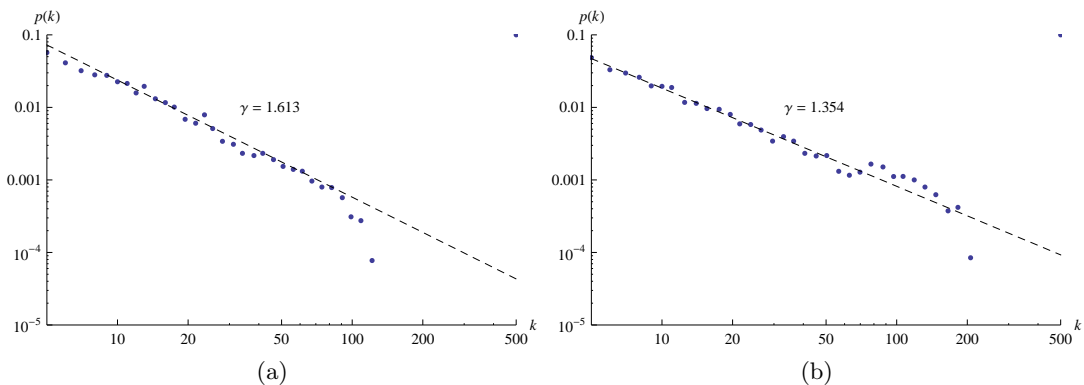


Figure 5.4: Subject Otago2. Log-log plot of the degree distribution of the functional brain network. Networks based on the Pearson correlation (5.3) with the threshold  $r = 0.9$  (a) rest phase (b) test phase.

To make the analysis complete, I have also studied the possibility of the emergence of a hierarchy in the functional brain networks (2.7). On the (*Fig. 5.6*) clustering distribution of the functional brain network of the subject Otago2 in rest and test phase is depicted. According to the distribution, there is no hierarchy present in the functional brain network. This is slightly surprising as there was hierarchicity discovered in anatomical human brain networks by modelling of interregional covariance in cortical thickness [11]. Moreover in contrary there was quite a strong hierarchicity of functional brain networks reported in [43]. I suppose that the hierarchy of functional brain networks should be studied more deeply also with the relation to the modularity of functional brain networks. As

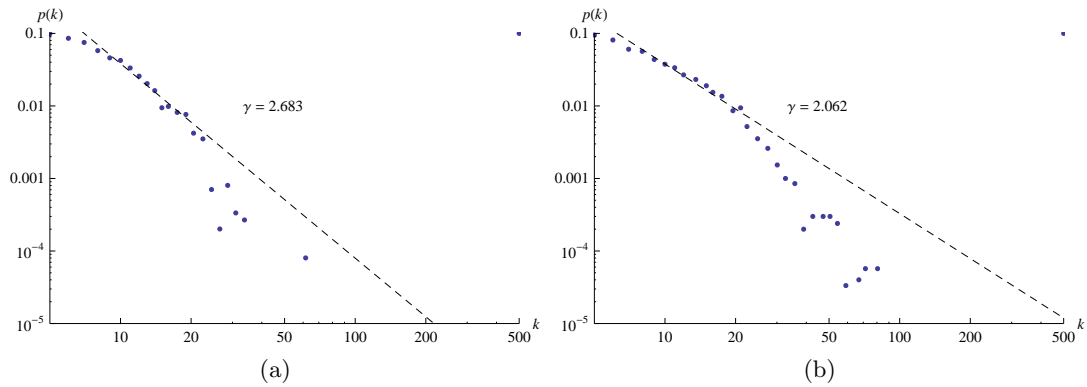


Figure 5.5: Subject Otago2. Log-log plot of the degree distribution of the functional brain network. Networks based on the Granger causality (5.6) with the threshold  $r = 50$  (a) rest phase (b) test phase.

has been shown in [43], modularity decomposition of functional brain networks seems to reflect the modularity of anatomical brain networks. These studies are still at the beginning.

Thus hierarchy of brain networks should be studied more deeply also with the relation to the modularity discovered in functional brain networks in rest. This organization reflects the known brain areas associated with specific functions [43].

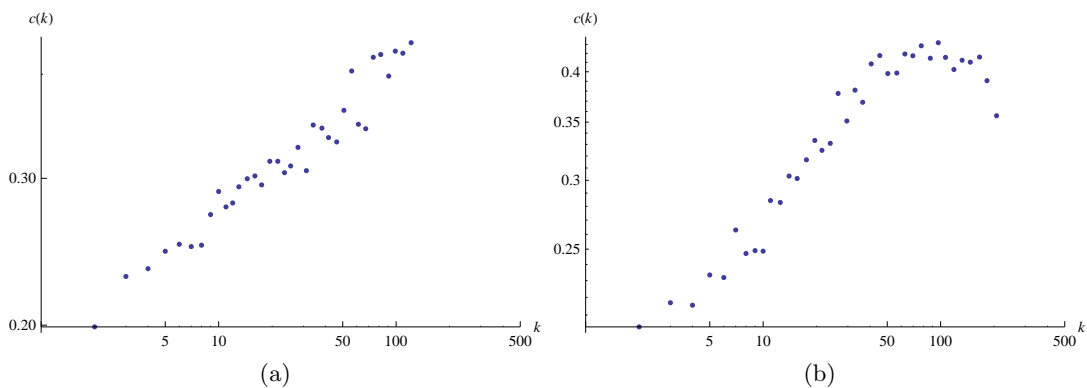


Figure 5.6: Log-log plot of the average clustering coefficient for a node degree of the functional brain network of the subject 'otago2'. Networks based on Pearson correlation (5.3) with the threshold  $r = 0.9$  (a) rest phase (b) test phase.

## 5.4 Functional brain networks and dementia

The limits of what functional brain networks are able to tell us are intensively studied. For example Buckner [14] presents a comprehensive fMRI study of young adults, nondemented older adults and demented adults. fMRI brain scans were taken while subjects were performing a simple sensory-motor task. They reported some differences between the fMRI data, but no systematic patterns or statistically significant differences were discovered. On the same data I have analyzed properties of functional brain networks. The results of this study are presented in next sections. As I have already mentioned, it is known that dementia affects the anatomical structure of a brain [8, 65]. The main question, I would like to answer is whether the functional brain networks will also reflect these changes.

### 5.4.1 Material and methods

fMRI data were gained from 44 subjects. 15 young adults (18-24 years) , 16 nondemented old adults (66-83 years) and 13 demented old adults(63-89). The cognitive task the people were asked to fulfill was simple finger tapping. Participants watched a transient large field 8Hz flickering checkerboard and pressed key at the onset of the flickering. 60 data acquisitions were made for each subject. In each test phase, scans in 8 timepoints were taken. Brains of participants were scanned only during the active phase. In each scan 65,536 voxels [(Z = 1 to 16 slices) ( $\tilde{X} = 64$ ) ( $\tilde{Y} = 64$ )] were measured (*Fig. 5.1*). I have averaged data from all 60 acquisitions to gain one functional brain network for each subject. From voxel intensities distributions (*Fig. 5.7*) have identified that the peak is at level of 500 units and selected voxels with the average intensity in range between 300 and 650 units which makes 15% - 18% of all voxels.

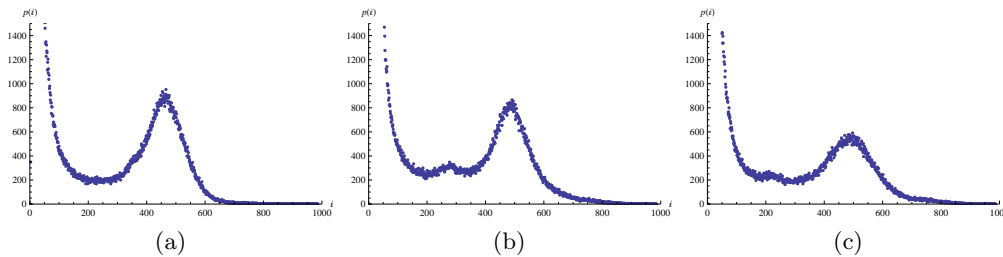


Figure 5.7: Distribution of average voxel intensities. (a) young people (b) old people(c) old people with dementia. Data were collected from all persons in a group. Peak is presented at value of 500 units. Voxels with intensities between 300 and 650 units were considered for functional brain networks.

I have generated two networks for each subject. I have used the Pearson cor-

relation (5.3) with the threshold  $r = 0.9$  and the Granger causality (5.6) with the threshold  $r = 80$ . These are the critical thresholds. After these values the generated networks became disconnected. For all generated networks I have calculated all relevant characteristics such as node separation (2.1), average clustering coefficient (2.5), degree and clustering distributions. All of them were calculated with the help of NWB tool [58].

### 5.4.2 Results

Measured parameters of all calculated networks are in Table A.1 (Appendix A). Calculation of the small-world index (2.8) for the networks based on Pearson correlation gives value around 20 showing that these networks have the small-world property. In the case of Granger causality, networks showed the same effect as described in the previous section. Average clustering coefficients are low ( $\sim 0.003$ ) showing a lack of small world structure.

In (*Fig. B.1 – B.4*) (Appendix B) and (*Fig. B.5 – B.7*) (Appendix B) degree distributions of all networks of all subjects are depicted. The scale-free power-law degree distribution (2.9) is present in all networks. However the difference among the groups is not quite obvious. There is a kind of tendency for younger subjects to have longer linear part in the log-log plot. But in each of the three groups (young, nondemented old and demented persons) there are exceptions from this behavior. To decide whether the effect has some significance, deeper statistical analysis is needed. The problem is that, the deeper statistical analysis requires more data, which is not easy to get. What can be told is that this tendency is more visible in networks created with a help of the Pearson correlation than those with the help of the Granger causality.

In agreement with the study of the data from the previous experiment, the clustering distribution did not follow the clustering distribution  $c(k) \propto k^{-\delta}$  (2.10) characteristic for the networks with a hierarchical structure. In (*Fig. 5.8*) is an example of this distribution for one subject of each group. There are lot of nodes with a high clustering coefficient and only a few with a small one.

## 5.5 Conclusions

In the first of my studies I have examined functional brain networks of four subjects, all of them were measured in two different conditions: during rest and during bimanual finger tapping task (test). I have revised [41] and made more detailed analysis of the data. In comparison to the original work I have considered all possible vector pairs as candidates for correlation links. I have also studied functional brain networks created with a help of the Granger causality. In the second study I have used Buckners fMRI dataset [14] and analyzed networks from 44 subjects of different ages, some of them with dementia. Only networks

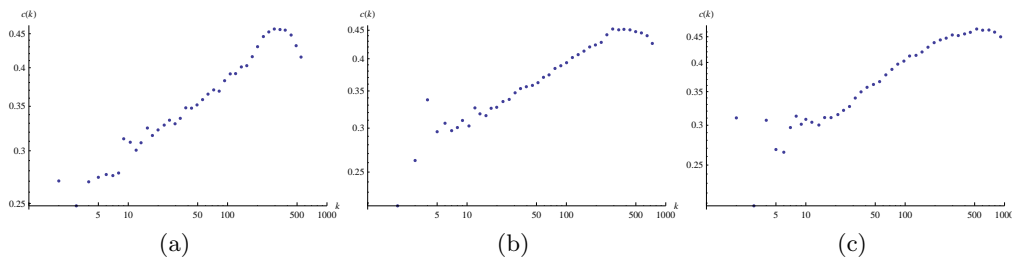


Figure 5.8: Log-log plot of the average clustering coefficient in relation to the node degree. (a) young subject (b) nondemented old (c) demented old. All networks created using Pearson correlation with the threshold  $r = 0.9$ .

generated with the help of the Pearson correlation (generated for all persons from both data sets) have the small-world property. Networks based on the Granger causality have a different structure with a much lower values of average clustering coefficient  $\sim 10^{-3}$  (2.5). Reason for this should be examined further. I have been expecting that the Granger causality describes the real dependency better as it takes also nonlinear dependencies into account, contrary to the Pearson correlation.

My results in relation to the scale-free property confirmed the results in [41]. However, the authors state that there is a possibility that functional brain networks have exponential and not power law degree distribution. Exponential degree distribution would follow a line in the log-linear plot. Networks I have created do not show this in log-linear plot (*Fig. 5.9*).

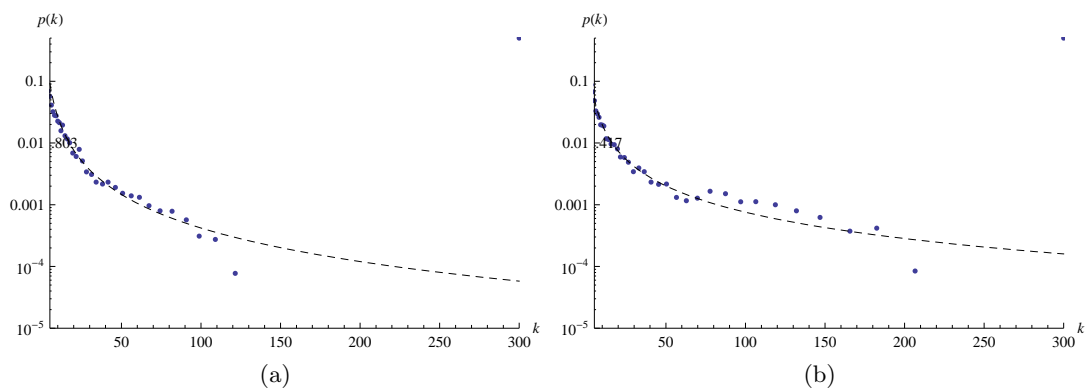


Figure 5.9: Log-linear plot of the degree distribution of the functional brain network of the subject 'otago2'. Networks created using Pearson correlation with the threshold  $r = 0.9$  (a) rest phase (b) test phase.

Amaral et al.[7] modelled network growth where the node degree expansion is constrained by node aging and cost limitations. They have shown that these constraints results in scale-free networks with a power law distribution and an exponentially decaying tail. Such a model seems to fit the degree distribution of studied functional brain networks and possibly explain the doubts about the power-law degree distribution mentioned in [41].

The differences between structure (mainly the degree distribution) of functional brain network of active, task performing brain and the brain in resting state were not too convincing. Neither were differences between functional networks between subjects having and not having dementia (see Appendix A)

In both cases I have shown that the clustering distribution (2.7) does not follow (2.10). This indicates a lack of hierarchy in the network [51]. On the other hand we have processed a raw data without any previous fMRI preprocessing. Recently a new technique based on the diffusion MRI was used to generate large, comprehensive white matter connectional datasets of the entire brain for two human subjects [32]. In this paper the question of the influence of data preprocessing on the final structure of functional brain networks was addressed.

The bimanual finger tapping task used for acquisition of Otago test data or motoric reaction to the blinking point used in the Buckner's experiment [14] are very simple cognitive tasks. The question is whether the structure and topology of functional brain network changes with a more demanding tasks. Or it is just more related to the anatomical connections and independent from the performed task? What is the relationship between anatomical brain networks and emerging functional brain networks is not clear. It is a task for the future studies, nevertheless first investigations show, that modular decomposition of functional brain networks might be helpful [43]. Latest studies [43] have shown that there is a modularity in the functional networks and that these modules correspond to the various regions in the brain responsible for different tasks.

Functional brain networks raised a lot of questions. Their investigations are at their beginning. There is even no agreement about the best way of extracting them. Latest studies [43] exhibit first attempts to retrieve necessary thresholds ( $r$ ) from the data and give more accurate mathematical basis of the network extraction. I see several possibilities how to continue functional brain network research:

1. Modular network decomposition and the question of its correspondence to the functional brain areas (visual cortex, motor cortex, etc.) is an interesting task to investigate. Relation between scale-free structure, modularity and hierarchy in functional brain networks can be also considered, possibly giving an answer on how the work of brain activity is organized.
2. To develop an exact mathematical basis of the network extraction. Then the functional brain network model can be created with a help of measured

data and network theory. Having such model, it would be possible to predict which areas are active in certain cognitive tasks.

The problem each such research faces, is the lack of the data. Scanners are usually possessed by hospitals and used for medical treatment. Those, which are in possession of scientific institutes are often beyond the reach, because the measurement time is expensive. Nevertheless, I hope, on the basis of cooperation with Liz Franz and Ľubica Benušková from University of Otago, Dunedin, New Zealand, to get more data to perform further analysis along the development of the theoretical methods and models. As we can see functional brain networks are complex networks with a structure which is not very well known. It is not sure what the best way to extract these networks from measured data is, and how to explain them. The debate on this subject continues [25, 43]. What I suppose, is that anatomical brain networks explain the functional networks and vice versa. To fulfill this goal a lot of studies are necessary. To create a good functional brain network model is an incredibly difficult task. Nevertheless, I suppose that such model can be developed in the future.

## Chapter 6

---

# Conclusions and discussion

---

Scientific methods give us possibility to study and design complex networks. Finding and measuring statistical properties such as node separation (2.1), clustering coefficient (2.5) or degree distribution (2.6) helps us to characterize the structure and behaviour of networks. Through the network models we can study the impact of these properties on the network evolution. We use mathematical and computational models to generate large networks and thus predict the future of real networks according measured parameters. Moreover, on the basis of suitable models, one is able to create network with properties desirable from the point of informatics for example. One is able to improve and develop fast search and navigation algorithms, design computer networks with a structure resistant to random failures or to place receivers and transmitters of the wireless network in the proper positions.

My thesis presents a combination of empirical work, measurements and experiments, and explanatory modelling and analysis of models. I and my co-workers have developed two theoretical models. First, the Word web model generates network with a similar statistical properties as the real positional word webs (Section 3.3). The other one, the clustering driven model (Section 4.2) includes a process that leads to the generation of scale-free hierarchical network. I have also presented experimental study of two real complex systems. The positional word web of several large texts (chapter 3) and the functional brain networks (Chapter 5).

Here I give the summary of my contributions in several areas covered by this thesis.

**Positional word web:** Together with my co-workers I have developed a model of growing network, that combines the preferential attachment (2.26) and the preferential edge rewiring (3.2). Networks generated by this model have small

world and scale-free structure. I am providing an analytical evidence, that degree distribution of these networks have two scaling regimes. The scaling exponent of the steeper part of the degree distribution can be modified through the parameters of the model (see chapter 3).

I have tested the validity of the model on the positional world web of The Bible. This was a natural choice, as the edge rewiring process was inspired by the words losing and gaining a new context in the language evolution. Our model [47] explains the difference between the exponent of the steeper part of the degree distribution predicted by the DM model [20] and the value measured by Cancho and Solé [15] in their positional word web. However, my numerical studies show that there is no evidence of two scaling regimes in the positional word web of The Bible. The same holds for the networks generated using our model. I have shown numerically that this is due to the network size, or due to the too big parameter  $c$  (3.2). The second regime appears in the network, if there are nodes with a degree higher than the  $k_{cross}$  parameter (3.8) (Fig. 3.3).

Measuring of clustering distribution (2.7) has shown that there is a hierarchical structure in all - real positional word web and generated networks (see Chapter 3).

**Clustering driven model:** I and my co-workers have used mechanism of preferential attachment to develop a clustering driven model of growing network (CD model) [4.2]. This model is based on preferential attachment driven by clustering coefficient and a local rule of adding edges to the nodes in selected cluster. A simplified version of this model can be compared to the Vázquez network with one surfer [62]. We have used the solution Vázquez random walk model to show analytically, that the scaling exponent of the degree distribution of the SCD model is  $\gamma = 3$  and is independent on the other parameters. To show this, I have used the solution of the Vázquez model we developed. I described this solution in Section (2.3.7). Furthermore, the CD model is a stochastic model that leads to the creation of a network with a weakly hierarchical structure (see Chapter 4).

In addition, we have shown that the clustering driven node addition itself is not responsible for the scale-free structure of a network. I agree with Vázquez, that independently on the node attachment kernel, local rules are decisive for the scale free property and hierarchy in the final network topology. It is due to the fact, that the local rule introduces effective preferential attachment [62] (see Chapter 4).

**Functional brain networks:** My work on functional brain networks involved studies of two datasets. For both I have constructed functional brain networks based on Pearson correlation (5.3) and Granger causality (5.6).

In the first study, I have examined functional brain networks of four subjects,

all of them were measured in two different conditions: during rest and during bimanual fingertapping task (test) [41]. I have revisited the paper [41] and made more detailed analysis of the data. In both conditions (rest and test), all generated functional brain networks have the small-world and the scale-free property. However, there was only a small difference in the length of the linear part of the degree distribution of functional brain networks of active, task performing brain and the brain in resting state (see Chapter 5).

In the second study I have used Buckners fMRI dataset [14] and analyzed networks from 44 subjects of different ages, some of them with dementia. The small world and scale-free property were present in generated networks as well.

In both cases, I have shown that the clustering distribution (2.7) does not follow  $c(k) \approx k^{-\delta}$  (2.10). This indicates a lack of hierarchy in the network [51].

My research has opened many questions and I have several ideas for the future investigation in the areas my research has addressed.

**Positional word web:** Positional word web networks studied in my work, were not large enough to show all properties of our model. Bigger real and generated networks should be studied to confirm the validity of the proposed model. We will try to find an analytical solution to determine the  $k_{cross}$  point. Later we can think about extending the model with further mechanisms. For example the parameter used for edge rewiring is a constant. But how will the model change when we rewire  $m_r t$  edges? Or how will the capacity of a node (number of neighbours the node can have) affect the generated networks. This effect is quite expected as the context of each word in language must be somehow limited.

**Clustering driven model:** In Chapter 4 I have shown our analytical solution of the simplified clustering driven model. But the analytical equations and solution of the original model is still unknown and further research is required. The clustering driven model has the ability to generate a scale-free structure thanks to the local rule of adding edges to a selected node and its neighbours. But how strict has this "locality" to be? What happens if we try to break it and add edges not to the closest neighbours but to the next closest neighbours? How far can we go before the network will lose its small-world and hierarchical structure?

**Functional brain networks:** Functional brain networks raised a lot of questions. Their studies are at the beginning. I can see several possibilities how to continue functional brain network research:

1. Tasks performed by subjects in my studies were easy from cognitive point of view. I expect that a more demanding task (reading or solving mathematical equations) can lead to differences in the structure of functional brain networks among different subjects and performed tasks. I hope, on

the basis of cooperation with Liz Franz and Ľubica Benušková from University of Otago, Dunedin, New Zealand, to get more data to perform further analysis.

2. Modular network decomposition and the question of its correspondence to the functional brain areas (visual cortex, motor cortex, etc.) can be studied. Relation between scale-free, modularity and hierarchy in functional brain networks should be investigated, possibly giving answer on how the brain activity is organized when the brain fulfills a cognitive task.
3. To build an exact mathematical basis of the network extraction. There is even no agreement about the best way of extracting them. Latest studies [43] exhibit first attempts to retrieve necessary thresholds ( $r$ ) based on accurate mathematical basis.
4. A long term goal is to find a network model that will explain the creation and evolution of functional brain networks.

Another part of complex network research is their visualization. I would like to develop algorithms that will display the networks in a way that expresses their scale-free structure, hierarchy or extract highly connected clusters. I believe that such visualization can help us to better understand the meaning of these properties and the processes that lead to creation of complex networks. For example visualization of functional brain networks can show the relation between the functional and anatomical structure of a brain.

In short, I would like to continue my research in building theoretical models, analyzing large scale real world networks and visualization of complex structures and processes that lead to their emergence.

---

# Bibliography

---

- [1] J. Abello, A. L. Buchsbaum, and J. R. Westbrook. A functional approach to external graph algorithms. In *Algorithmica*, pages 332–343. Springer-Verlag, 1998.
- [2] S. Achard, R. Salvador, B. Whitcher, J. Suckling, and E. Bullmore. A resilient, low-frequency, small-world human brain functional network with highly connected association cortical hubs. *The Journal of neuroscience : the official journal of the Society for Neuroscience*, 26(1):63–72, January 2006.
- [3] R. Albert and A. L. Barabási. Statistical mechanics of complex networks. *Reviews of Modern Physics*, 74(1):47–97, January 2002.
- [4] R. Albert, H. Jeong, and A. L. Barabási. The diameter of the world wide web. *Nature*, 401:130–131, 1999.
- [5] R. Albert, H. Jeong, and A. L. Barabási. Error and attack tolerance of complex networks. *Nature*, 406(6794):378–382, July 2000.
- [6] E. Almaas and A. L. Barabási. Power laws in biological networks, 2004.
- [7] L. A. Amaral, A. Scala, M. Barthelemy, and H. E. Stanley. Classes of small-world networks. *Proceedings of the National Academy of Sciences of the United States of America*, 97(21):11149–11152, October 2000.
- [8] J. Appel, E. Potter, Q. Shen, G. Pantol, Maria T. Greig, D. Loewenstein, and R. Duara. A comparative analysis of structural brain mri in the diagnosis of alzheimer’s disease. *Behavioural neurology*, 21(1):13–19, 2009.
- [9] A. L. Barabási and R. Albert. Emergence of scaling in random networks. *Science (New York, N.Y.)*, 286(5439):509–512, October 1999.
- [10] A. L. Barabási, H. Jeong, Z. Neda, E. Ravász, A. Schubert, and T. Vicsek. Evolution of the social network of scientific collaborations. *Physica A: Statistical Mechanics and its Applications*, 311(3-4):590 – 614, April 2002.
- [11] D. S. Bassett, E. Bullmore, B. A. Verchinski, V. S. Mattay, D. R. Weinberger, and A. Meyer-Lindenberg. Hierarchical organization of human cortical networks in health and schizophrenia. *J. Neurosci.*, 28(37):9239–9248, 2008.
- [12] <http://unbound.biola.edu>.

- [13] Béla Bollobas. *Random Graphs*. Cambridge University Press, January 2001.
- [14] R. L. Buckner, A. Z. Snyder, A. L. Sanders, M. E. Raichle, and J. C. Morris. Functional brain imaging of young, nondemented, and demented older adults. *J. Cognitive Neuroscience*, 12(Supplement 2):24–34, 2000.
- [15] R. F. Cancho and R. V. Solè. The small world of human language. *Proceedings of The Royal Society of London. Series B, Biological Sciences*, 268:2261–2266, 2001.
- [16] D. R. Chialvo. Critical brain networks. *Physica A*, 340(4):756–765, 2004.
- [17] F. Chung and L. Lu. The diameter of sparse random graphs. *Adv. Appl. Math.*, 26(4):257–279, 2001.
- [18] R. Diestel. *Graph Theory*, volume 173 of *Graduate Texts in Mathematics*. Springer-Verlag, Heidelberg, second edition, 2000.
- [19] S. Dodel, M. J. Herrmann, and T. Geisel. Functional connectivity by cross-correlation clustering. *Neurocomputing*, 44-46:1065–1070, June 2002.
- [20] S. N. Dorogovtsev and Mendés J. F. F. Language as an evolving word web. *Proc.Royal Soc.London B*, 268:2603, 2001.
- [21] S. N. Dorogovtsev and J. F. F. Mendés. Effect of the accelerating growth of communications networks on their structure. *Physical Review E*, 63:025101, 2001.
- [22] S. N. Dorogovtsev and J. F. F. Mendés. Scaling properties of scale-free evolving networks: Continuous approach. *Physical Review E*, 63:056125, 2001.
- [23] S. N. Dorogovtsev and J. F. F. Mendés. *Evolution of Networks: From Biological Nets to the Internet and WWW (Physics)*. Oxford University Press, USA, March 2003.
- [24] S. N. Dorogovtsev, J. F. F. Mendés, and A. N. Samukhin. Structure of growing networks with preferential linking. *Phys Rev Lett*, 85(21):4633–4636, November 2000.
- [25] V. M. Eguíluz, D. R. Chialvo, G. A. Cecchi, M. Baliki, and A. V. Apkarian. Scale-free brain functional networks. *Phys Rev Lett*, 94(1), January 2005.
- [26] P. Erdős and A. Rényi. On random graphs, i. *Publicationes Mathematicae (Debrecen)*, 6:290–297, 1959.
- [27] M. Faloutsos, P. Faloutsos, and Ch. Faloutsos. On power-law relationships of the internet topology. In *SIGCOMM '99: Proceedings of the conference on Applications, technologies, architectures, and protocols for computer communication*, volume 29, pages 251–262, New York, NY, USA, October 1999. ACM.
- [28] Paola Flocchini, Rastislav Královič, Peter Ružička, Alessandro Roncato, and Nicola Santoro. On time versus size for monotone dynamic monopolies in regular topologies. *J. of Discrete Algorithms*, 1(2):129–150, 2003.
- [29] <https://pantherfile.uwm.edu/neuropsych/www/fmri.html>.

- [30] C. W. J. Granger. Investigating causal relations by econometric models and cross-spectral methods. *Econometrica*, 37(3):424–438, 1969.
- [31] <http://www.gutenberg.org>.
- [32] P. Hagmann, M. Kurant, X. Gigandet, P. Thiran, V. J. Wedeen, R. Meuli, and J. P. Thiran. Mapping human whole-brain structural networks with diffusion mri. *Plos One*, 7(2):e597, July 2007.
- [33] S.A. Huettel, A. W. Song, and G. McCarthy. *Functional Magnetic Resonance Imaging, 2nd Edition*. Sinauer Associates, January 2009.
- [34] M.D Humphries, K Gurney, and T.J Prescott. The brainstem reticular formation is a small-world, not scale-free, network. *Proceedings of the Royal Society B: Biological Sciences*, 273(1585):503–511, 2006.
- [35] F. Karinthy. Chain-links, 1929.
- [36] Jon Kleinberg. The small-world phenomenon: an algorithm perspective. In *STOC '00: Proceedings of the thirty-second annual ACM symposium on Theory of computing*, pages 163–170, New York, NY, USA, 2000. ACM.
- [37] M. Kochen. *The Small World*. Norwood, NJ: Ablex, 1989.
- [38] Markošová M. and Náther P. Language as a graph (in slovak). *Mind, Intelligence and Life*, pages 298–307, 2007.
- [39] M. Markošová. Dynamika sietí. In *Umelá Inteligencia a kognitívna veda II*. prepared for printing, 2010. Editors: Kvasnička, V. and Pospíchal J.
- [40] M. Markošová. Network model of human language. *Physica A: Statistical Mechanics and its Applications*, 387:661–666, January 2008.
- [41] M. Markošová, L. Franz, and L. Benušková. Topology of brain functional networks: Towards the role of genes. In *ICONIP (1)*, pages 111–118, 2008.
- [42] M. Markošová and P. Náther. Language as a small world network. *Hybrid Intelligent Systems, International Conference on*, 0:37, 2006.
- [43] D. Meunier, R. Lambiotte, A. Fornito, K. D. Ersche, and E. T. Bullmore. Hierarchical modularity in human brain functional networks. *Frontiers in neuroinformatics*, 3, 2009.
- [44] S. Milgram. The small world problem. *Psychology Today*, 1:61, 1967.
- [45] Q. D. Morris, B. J. Frey, and Ch. J. Paige. Denoising and untangling graphs using. In *Proc. Neural Info. Proc. Sys*, page 2003, 2003.
- [46] A. E. Motter, de Moura A. P. S., Y. Lai, and P. Dasgupta. Topology of the conceptual network of language. *Physical Review E*, 65:065102, 2002.
- [47] P. Náther and M. Markošová. Positional word web and its numerical and analytical studies. prepared for publication, 2010.

- [48] P. Náther, M. Markošová, and B. Rudolf. Hierarchy in the growing scale-free network with local rules. *Physica A Statistical Mechanics and its Applications*, 388:5036–5044, December 2009.
- [49] A. S. Nencka and D. B. Rowe. Reducing the unwanted draining vein bold contribution in fmri with statistical post-processing methods. *Neuroimage*, 37(1):177–88, 2007.
- [50] R. Pastor-Satorras and A. Vespignani. *Evolution and Structure of the Internet: A Statistical Physics Approach*. Cambridge University Press, New York, NY, USA, 2004.
- [51] E. Ravász and A. L. Barabási. Hierarchical organization in complex networks. *Phys Rev E Stat Nonlin Soft Matter Phys*, 67(2 Pt 2), February 2003.
- [52] E. Ravász, A. L. Somera, D. A. Mongru, Z. N. Oltvai, and A. L. Barabási. Hierarchical organization of modularity in metabolic networks. *Science*, 297(5586):1551–1555, August 2002.
- [53] A. Roebroeck, E. Formisano, and R. Goebel. Mapping directed influence over the brain using granger causality and fmri. *NeuroImage*, 25(1):230–242, March 2005.
- [54] L. A. Schintler, A. Reggiani, R. Kulkarni, and Nijkamp P. Scale-free phenomena in communication networks: A cross-atlantic comparison, August 2003.
- [55] J. R. Stroop. Studies of interference in serial verbal reactions. *Journal of Experimental Psychology*, 18(6):643–662, 1935.
- [56] J. C. Tamraz, Y.G. Comair, and H.O. Luders. *Atlas of Regional Anatomy of the Brain Using MRI: With Functional Correlations*. Springer-Verlag, April 2004.
- [57] Ch. Tantipathananandh, T. Berger-Wolf, and Kempe D. A framework for community identification in dynamic social networks. In *KDD '07: Proceedings of the 13th ACM SIGKDD international conference on Knowledge discovery and data mining*, pages 717–726, New York, NY, USA, 2007. ACM.
- [58] NWB Team. Network workbench tool, 2006.
- [59] H. P. Thadakamalla, R. Albert, and S. R. T. Kumara. Search in spatial scale-free networks. *New Journal of Physics*, 9(6):190, 2007.
- [60] Ch. K. Tse, X. Liu, and M. Small. Analyzing and composing music with complex networks: finding structures. In *in Bach[U+FFFD]s, Chopin[U+FFFD]s and Mozart[U+FFFD]s, [U+FFFD] International Symposium on Nonlinear Theory and Its Applications, (NOLTA2008)*, 2008.
- [61] M. Vandenheuvel, C. Stam, M. Boersma, and H. Hulshoffpol. Small-world and scale-free organization of voxel-based resting-state functional connectivity in the human brain. *NeuroImage*, 43(3):528–539, November 2008.
- [62] A. Vázquez. Growing network with local rules: Preferential attachment, clustering hierarchy, and degree correlations. *Physical Review E*, 67(5):056104+, May 2003.

- [63] D. J. Watts. *Small worlds: The dynamics of networks between order and randomness*. Princeton University Press, Princeton, NJ, 1999.
- [64] D. J. Watts and S. H. Strogatz. Collective dynamics of 'small-world' networks. *Nature*, 393(6684):440–442, June 1998.
- [65] K. A. Welsh-Bohmer and III White, Ch. L. Alzheimer disease: What changes in the brain cause dementia? *Neurology*, 72(4):e21–, 2009.
- [66] Ye Xu and W. Zhuo. On a model of internet topology structure. *Multimedia Information Networking and Security, International Conference on*, 1:378–382, 2009.
- [67] H. Zhang, A. Goel, and R. Govindan. Using the small-world model to improve freenet performance. *Comput. Netw.*, 46(4):555–574, 2004.
- [68] H. Zhu and Z. Huang. Navigation in a small world with local information. *Physical Review E*, 70:036117, 2004.

# Appendices

## Appendix A

---

# Appendix A

---

Table A.1: Properties of all complex networks used in this thesis. Here  $N$  is the number of nodes,  $\bar{c}$  is the average clustering coefficient (2.5),  $\ell$  is the node separation (2.1),  $\bar{k}$  the average node degree,  $\gamma$  the degree distribution scaling coefficient (2.9),  $\delta$  the scaling coefficient of the clustering distribution (2.10) pointing to hierarchicity.

network	$N$	$\bar{c}$	$\ell$	$\bar{k}$	$\gamma$	$\delta$
language word webs and generated networks						
drv	11379	0.772	2.18	46	1.674	1.300
asv	10076	0.768	2.18	46	1.654	1.272
nrsv	14716	0.718	2.24	50	1.651	1.249
bev	4942	0.764	2.12	60	1.325	1.348
kjv	11592	0.771	2.18	47	1.659	1.296
prg	21104	0.700	2.27	49	1.970	1.238
kjvGen	11592	0.093	2.76	42	1.644	0.422
kjvGenME	11592	0.234	2.72	45	1.717	0.558
prgGen	21104	0.085	2.81	45	1.752	0.523
prgGenME	21104	0.166	2.80	47	1.743	0.594
gen20000	20000	0.002	3.79	13	1.50, 3.53	
clustering driven models						
SCD model	20000	0.730	6.88	4	2.995	1.000
CD model	20000	0.627	5.60	6	2.916	0.973
Random model	20000	0.658	7.24	6	2.988	0.955

network	$N$	$\bar{c}$	$\ell$	$\bar{k}$	$\gamma$	$\delta$
functional brain networks - test vs rest study - fMRI Otago data						
otago1-pearson-0.9-rest	4901	0.375	5.49	35	1.370	
otago1-pearson-0.9-test	4869	0.289	7.41	12	1.193	
otago2-pearson-0.9-rest	4302	0.262	6.77	11	1.803	
otago2-pearson-0.9-test	4304	0.283	5.99	21	1.417	
otago3-pearson-0.9-rest	3446	0.246	8.77	5	3.257	
otago3-pearson-0.9-test	3491	0.245	9.75	5	1.848	
otago4-pearson-0.9-rest	3819	0.263	7.14	8	2.031	
otago4-pearson-0.9-test	3834	0.267	7.87	9	2.106	
otago1-granger-50-rest	5517	0.002	4.71	18	1.961	
otago1-granger-50-test	5534	0.001	5.07	8	2.950	
otago2-granger-50-rest	4978	0.001	5.38	6	3.185	
otago2-granger-50-test	5000	0.002	5.00	8	3.219	
otago2-granger-50-rest	4279	0.0009	6.15	5	5.667	
otago3-granger-50-test	4291	0.001	5.98	5	5.324	
otago4-granger-50-rest	4389	0.001	5.55	6	4.326	
otago4-granger-50-test	4452	0.001	5.66	5	5.294	
functional brain networks - dementia study						
young1-pearson-0.9	10222	0.345	4.06	86	1.405	
young2-pearson-0.9	11423	0.332	4.07	84	1.471	
young3-pearson-0.9	9040	0.356	4.04	86	0.997	
young4-pearson-0.9	10850	0.326	4.14	67	1.289	
young5-pearson-0.9	11519	0.333	4.06	86	1.281	
young6-pearson-0.9	11808	0.349	3.89	124	1.179	
young7-pearson-0.9	9337	0.339	4.13	75	1.318	
young8-pearson-0.9	13741	0.315	4.10	64	0.958	
young9-pearson-0.9	10420	0.338	4.07	81	1.271	
young10-pearson-0.9	11206	0.327	4.08	79	1.528	
young11-pearson-0.9	11275	0.350	3.94	111	1.235	
young12-pearson-0.9	11466	0.336	4.05	79	1.141	
young13-pearson-0.9	10915	0.396	3.75	181	0.857	
young14-pearson-0.9	8867	0.337	4.18	67	1.353	
nondemented1-pearson-0.9	3177	0.414	4.34	42	0.821	
nondemented2-pearson-0.9	10429	0.378	3.83	132	0.865	
nondemented3-pearson-0.9	9194	0.421	3.64	203	0.768	
nondemented4-pearson-0.9	12044	0.351	3.91	108	0.903	
nondemented5-pearson-0.9	9449	0.388	3.85	131	0.898	

network	$N$	$\bar{c}$	$\ell$	$\bar{k}$	$\gamma$	$\delta$
nondemented6-pearson-0.9	9253	0.375	3.86	118	0.972	
nondemented7-pearson-0.9	11101	0.338	4.04	89	1.175	
nondemented8-pearson-0.9	9034	0.382	3.85	142	0.999	
nondemented9-pearson-0.9	9714	0.425	3.66	221	0.911	
nondemented10-pearson-0.9	10289	0.317	4.20	49	1.265	
nondemented11-pearson-0.9	12104	0.326	4.10	65	0.893	
nondemented12-pearson-0.9	10286	0.356	3.95	119	1.285	
nondemented13-pearson-0.9	10768	0.367	3.88	114	0.857	
nondemented14-pearson-0.9	10188	0.419	3.75	224	0.989	
nondemented15-pearson-0.9	10293	0.353	3.97	91	1.087	
demented1-pearson-0.9	11024	0.425	3.62	198	0.616	
demented2-pearson-0.9	8372	0.325	4.30	43	1.196	
demented3-pearson-0.9	9618	0.366	3.93	96	0.884	
demented4-pearson-0.9	8082	0.395	3.85	114	0.754	
demented5-pearson-0.9	11181	0.382	3.78	170	1.020	
demented6-pearson-0.9	11196	0.416	3.64	201	0.648	
demented7-pearson-0.9	11768	0.346	3.97	100	1.082	
demented8-pearson-0.9	9249	0.366	3.91	98	0.859	
demented9-pearson-0.9	7967	0.349	4.08	69	1.008	
demented10-pearson-0.9	8949	0.348	4.05	75	1.092	
demented11-pearson-0.9	9381	0.362	3.97	90	0.917	
demented12-pearson-0.9	9639	0.316	4.23	44	1.130	
nondemented1-granger-80.0	3178	0.005	4.45	10	3.878	
nondemented2-granger-80.0	10436	0.003	3.37	42	1.026	
nondemented3-granger-80.0	9200	0.004	3.26	48	0.989	
nondemented4-granger-80.0	12045	0.003	3.38	34	1.273	
nondemented5-granger-80.0	9453	0.003	3.46	38	1.281	
nondemented6-granger-80.0	9255	0.004	3.54	31	1.320	
nondemented7-granger-80.0	11101	0.003	3.52	27	1.597	
nondemented8-granger-80.0	9037	0.004	3.40	32	1.298	
nondemented9-granger-80.0	9724	0.004	3.28	42	1.170	
nondemented10-granger-80.0	10290	0.002	3.71	21	2.016	
nondemented11-granger-80.0	12104	0.003	3.57	28	1.363	
nondemented12-granger-80.0	10288	0.003	3.59	25	1.754	
nondemented13-granger-80.0	10769	0.004	3.39	33	1.265	
nondemented14-granger-80.0	10194	0.005	3.41	35	1.286	
nondemented15-granger-80.0	10297	0.002	3.57	28	1.430	
demented1-granger-80.0	11036	0.004	3.18	53	0.934	

network	$N$	$\bar{c}$	$\ell$	$\bar{k}$	$\gamma$	$\delta$
demented2-granger-80.0	8372	0.003	3.81	18	2.475	
demented3-granger-80.0	9626	0.003	3.52	28	1.403	
demented4-granger-80.0	8090	0.003	3.60	25	1.413	
demented5-granger-80.0	11178	0.003	3.39	33	1.276	
demented6-granger-80.0	11203	0.004	3.17	58	0.939	
demented7-granger-80.0	11769	0.003	3.47	31	1.368	
demented8-granger-80.0	9254	0.003	3.55	25	1.568	
demented9-granger-80.0	7973	0.002	3.69	20	1.865	
demented10-granger-80.0	8949	0.003	3.65	22	1.897	
demented11-granger-80.0	9390	0.003	3.49	27	1.516	
demented12-granger-80.0	9640	0.002	3.63	22	1.687	

## Appendix B

---

# Appendix B

---

Figures B.1 - B.4 and B.5 - B.7 display log-log plots of degree distributions of all subjects from the dementia study, divided into three groups (young, nondemented, demented) for networks created using Pearson correlation and Granger causality.

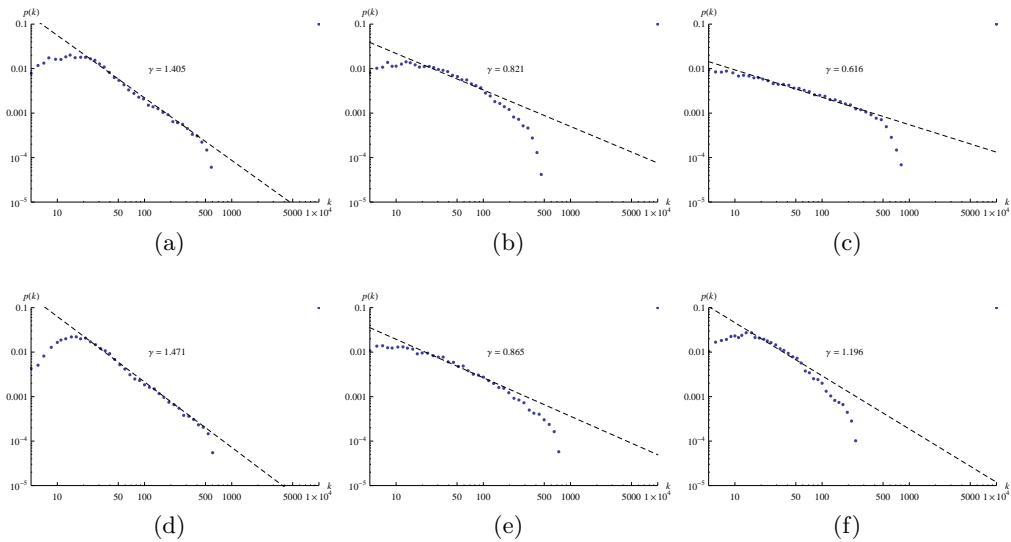


Figure B.1: Log-log plot of the degree distribution of all subjects from the dementia study divided into young (left), nondemented old (center) and demented old (right). All networks created using Pearson correlation with the threshold  $r = 0.9$ .

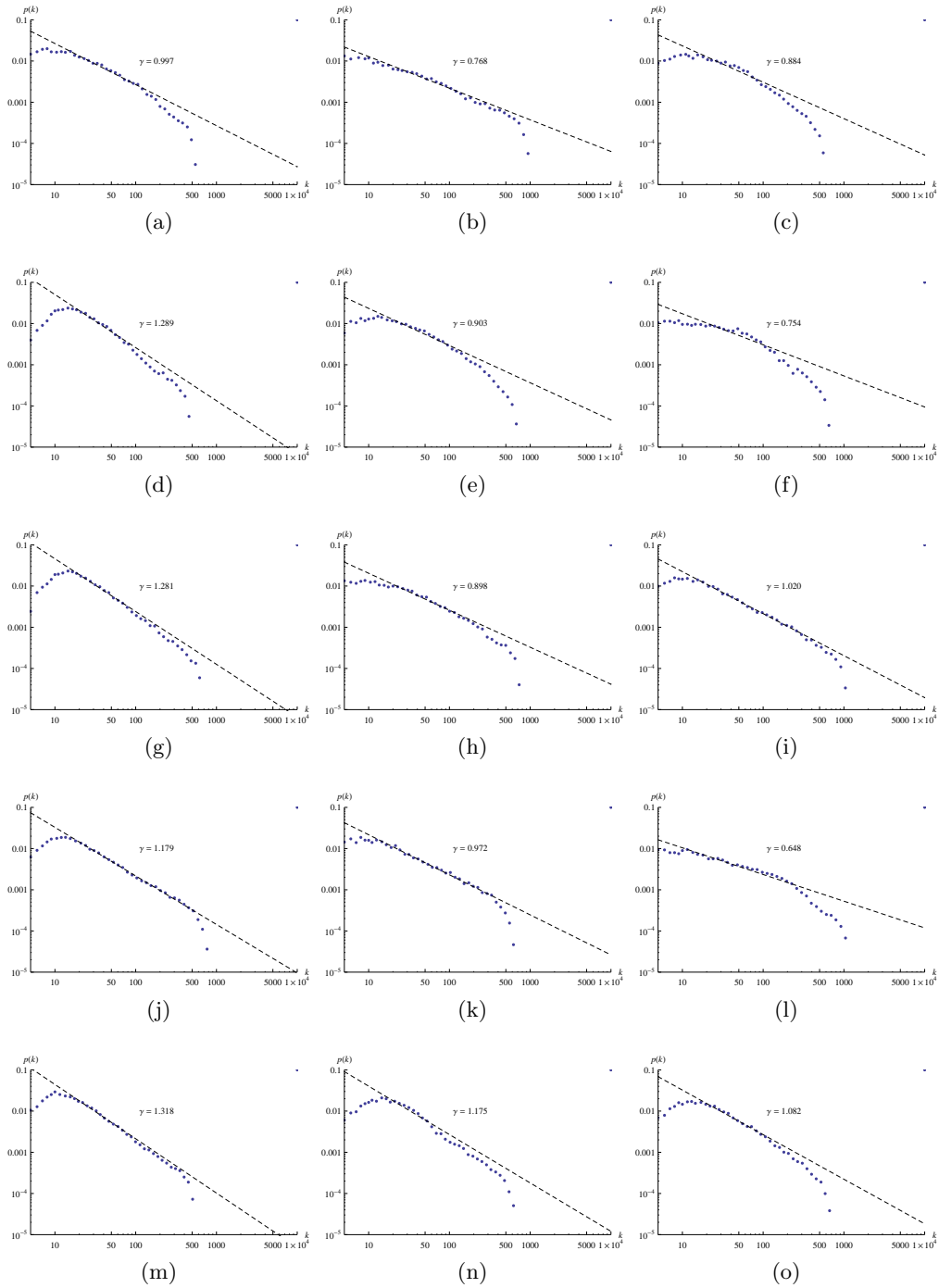


Figure B.2: Log-log plot of the degree distribution of all subjects from the dementia study divided into young (left), nondemented old (center) and demented old (right). All networks created using Pearson correlation with the threshold  $r = 0.9$ .

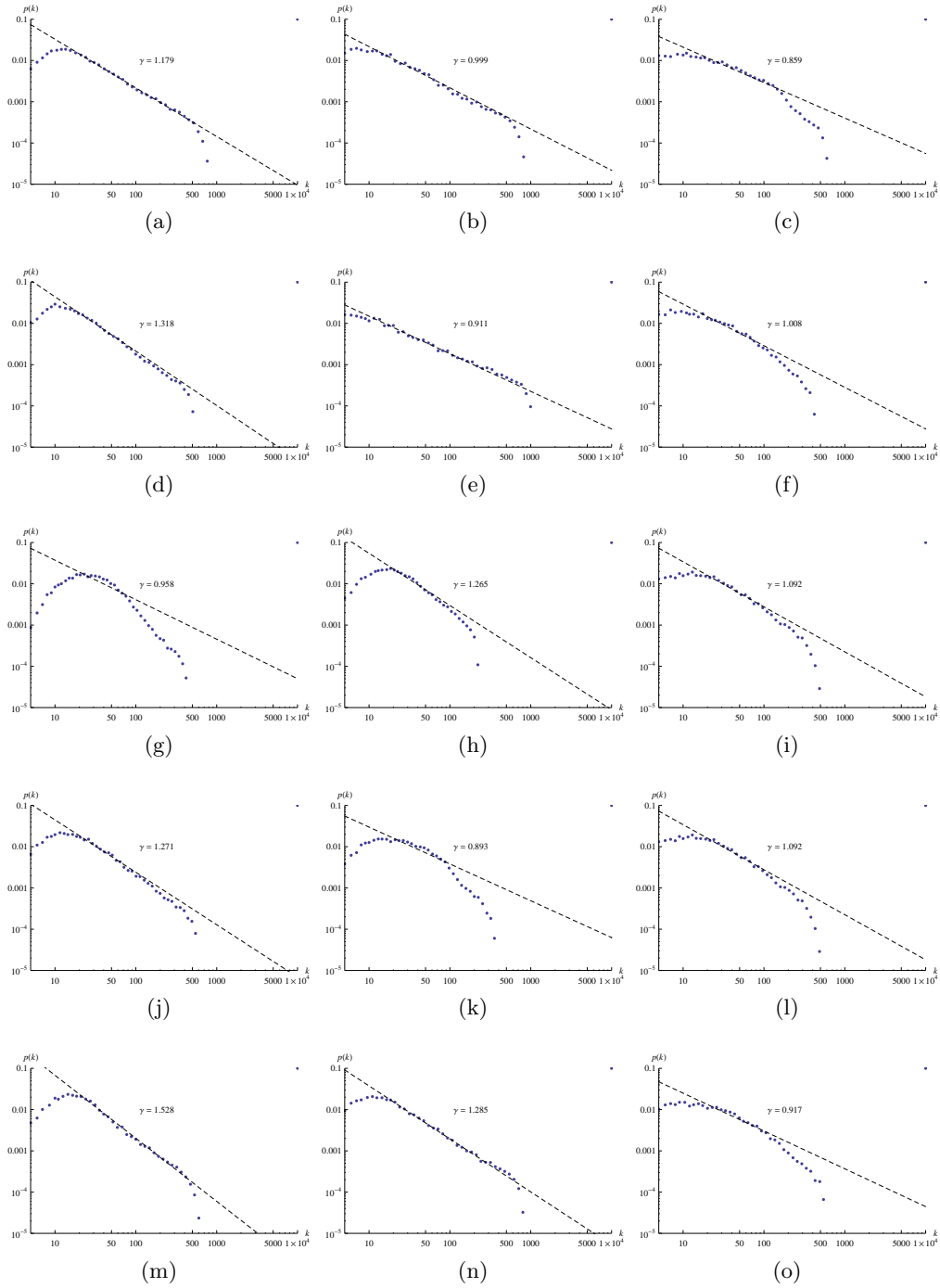


Figure B.3: Log-log plot of the degree distribution of all subjects from the dementia study divided into young (left), nondemented old (center) and demented old (right). All networks created using Pearson correlation with the threshold  $r = 0.9$ .

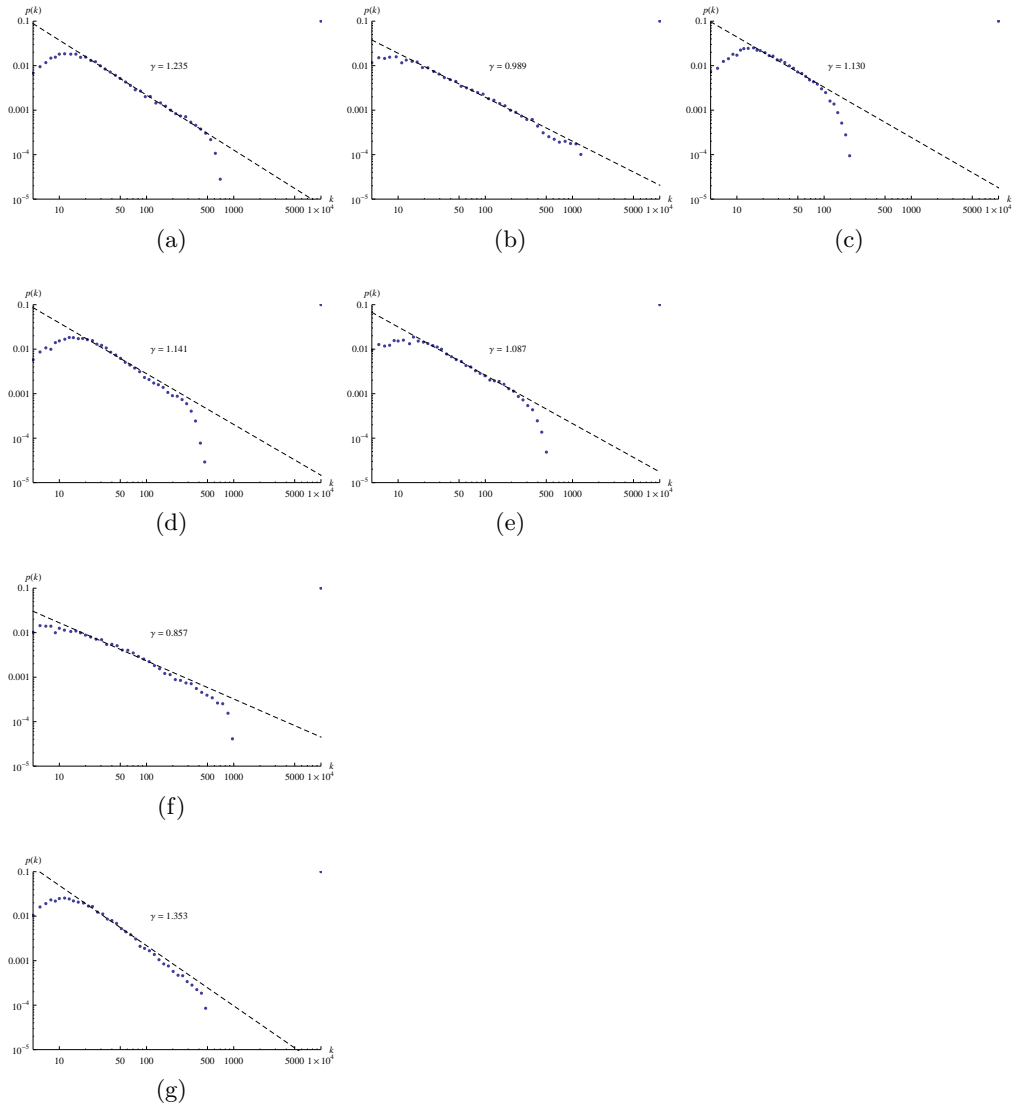


Figure B.4: Log-log plot of the degree distribution of all subjects from the dementia study divided into young (left), nondemented old (center) and demented old (right). All networks created using Pearson correlation with the threshold  $r = 0.9$ .

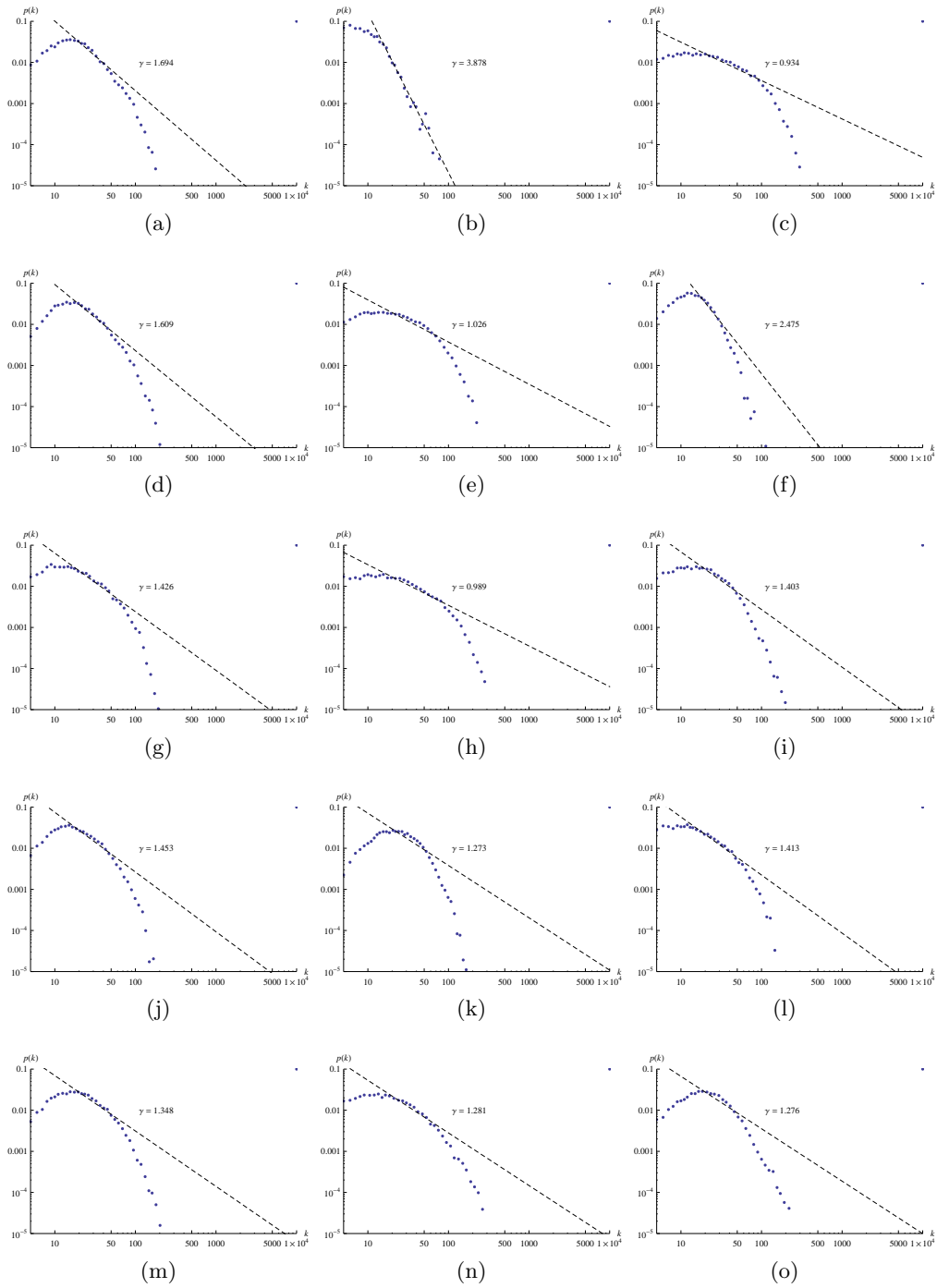


Figure B.5: Log-log plot of the degree distribution of all subjects from the dementia study divided into young (left), nondemented old (center) and demented old (right). All networks created using Granger causality with the threshold  $r = 80$ .

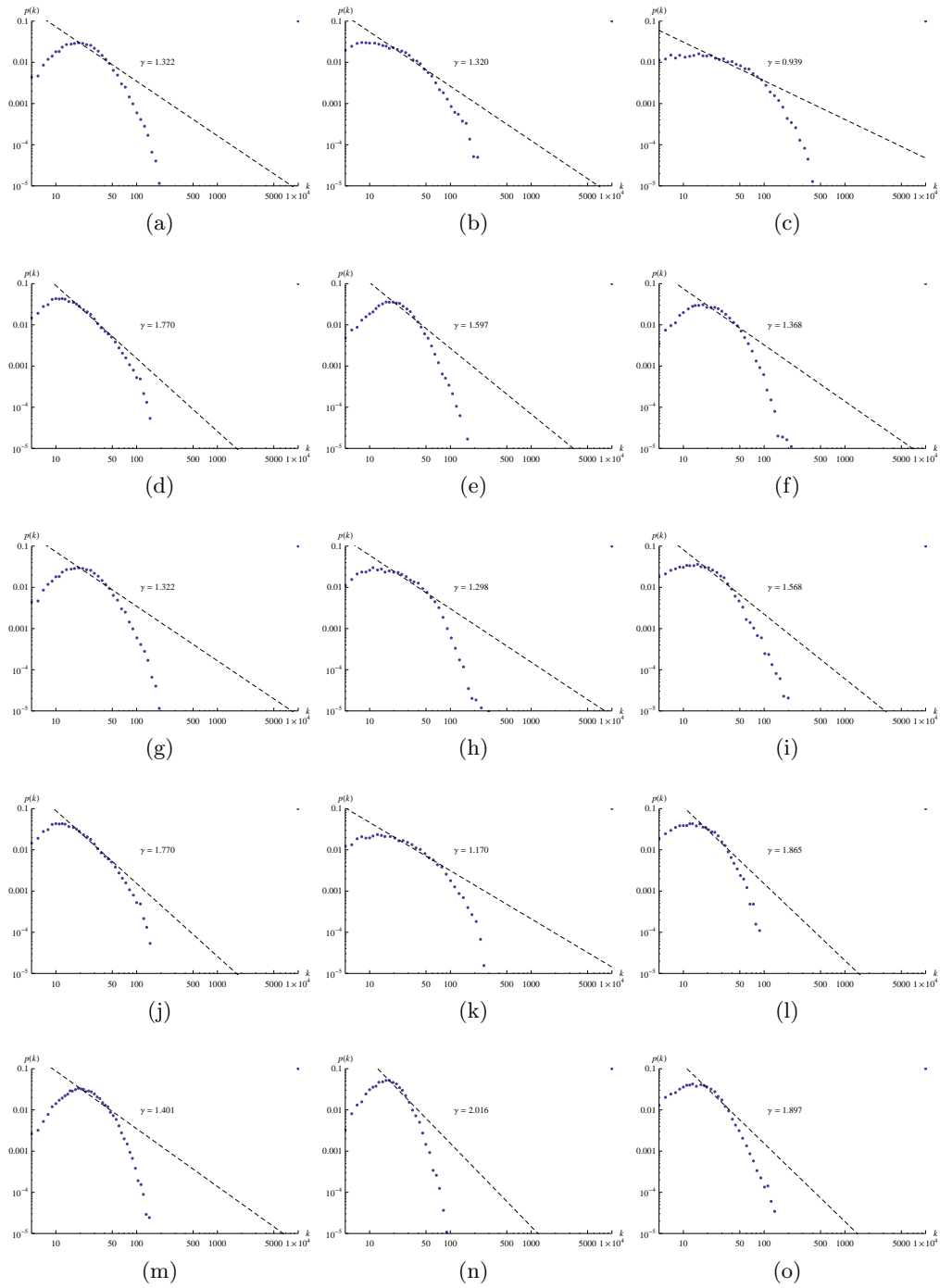


Figure B.6: Log-log plot of the degree distribution of all subjects from the dementia study divided into young (left), nondemented old (center) and demented old (right). All networks created using Granger causality with the threshold  $r = 80$ .

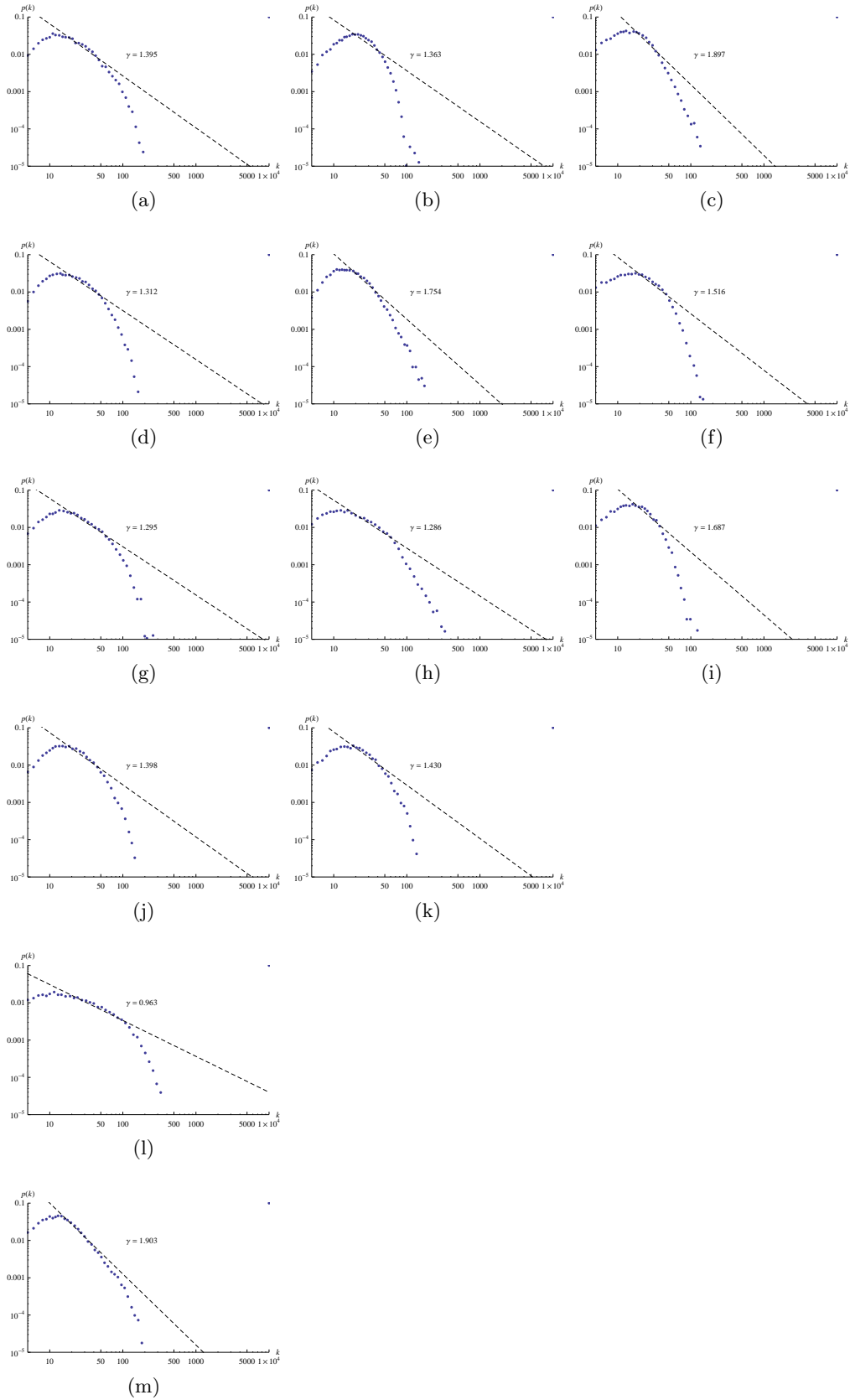


Figure B.7: Log-log plot of the degree distribution of all subjects from the dementia study divided into young (left), nondemented old (center) and demented old (right). All networks created using Granger causality with the threshold  $r = 80$ .